Lecture 16

Supernova Light Curves and Spectra

Normal Core-Collapse Supernovae

SN 1994D

Supernova – the explosive death of an entire star –*

currently active supernovae are given at

http://www.rochesterastronomy.org/supernova.html

* *Usually, you only die once*

Basic spectroscopic classification of supernovae

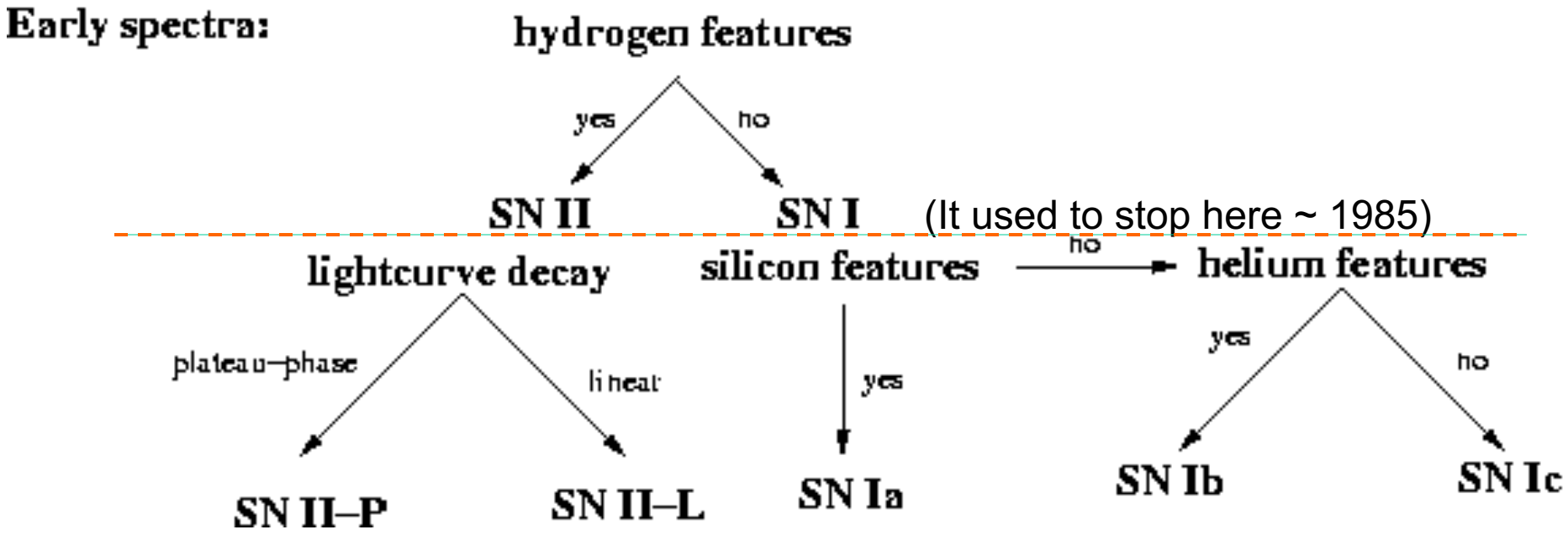

Also II b, II n, Ic –bl, I-pec, 87A-like, SLSN, imposters, etc.

The spectrum at peak depends on the properties of the star that blew up, especially whether it had a hydrogen envelope or not. Obviously white dwarfs and Wolf-Rayet stars don't (or have very little)

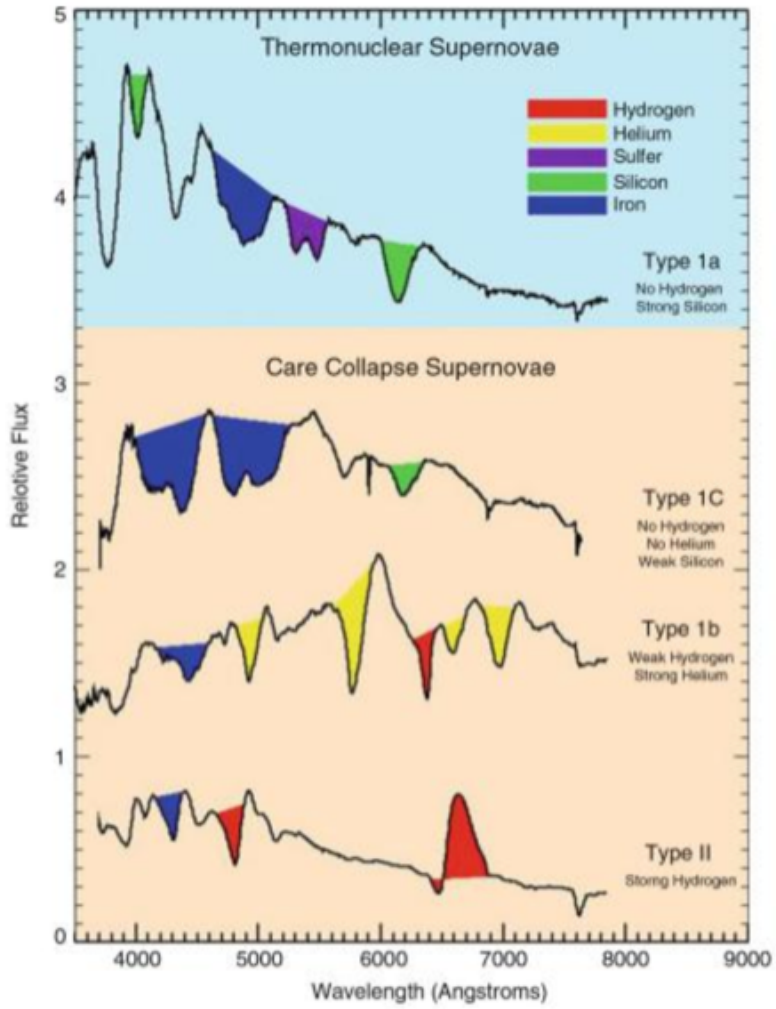

Model-wise, all Type II supernovae and Ib and Ic as well as SLSN come from massive stars.

Type Ia and subclasses thereof come from exploding white dwarfs.

The "red" H on the SN Ib at the left is not common.

Generally, but not always two things make a supernova bright – large radius (supergiants, SN II) or lots of radioactivity (SN I)

The faintness of 87A is exaggerated in this plot

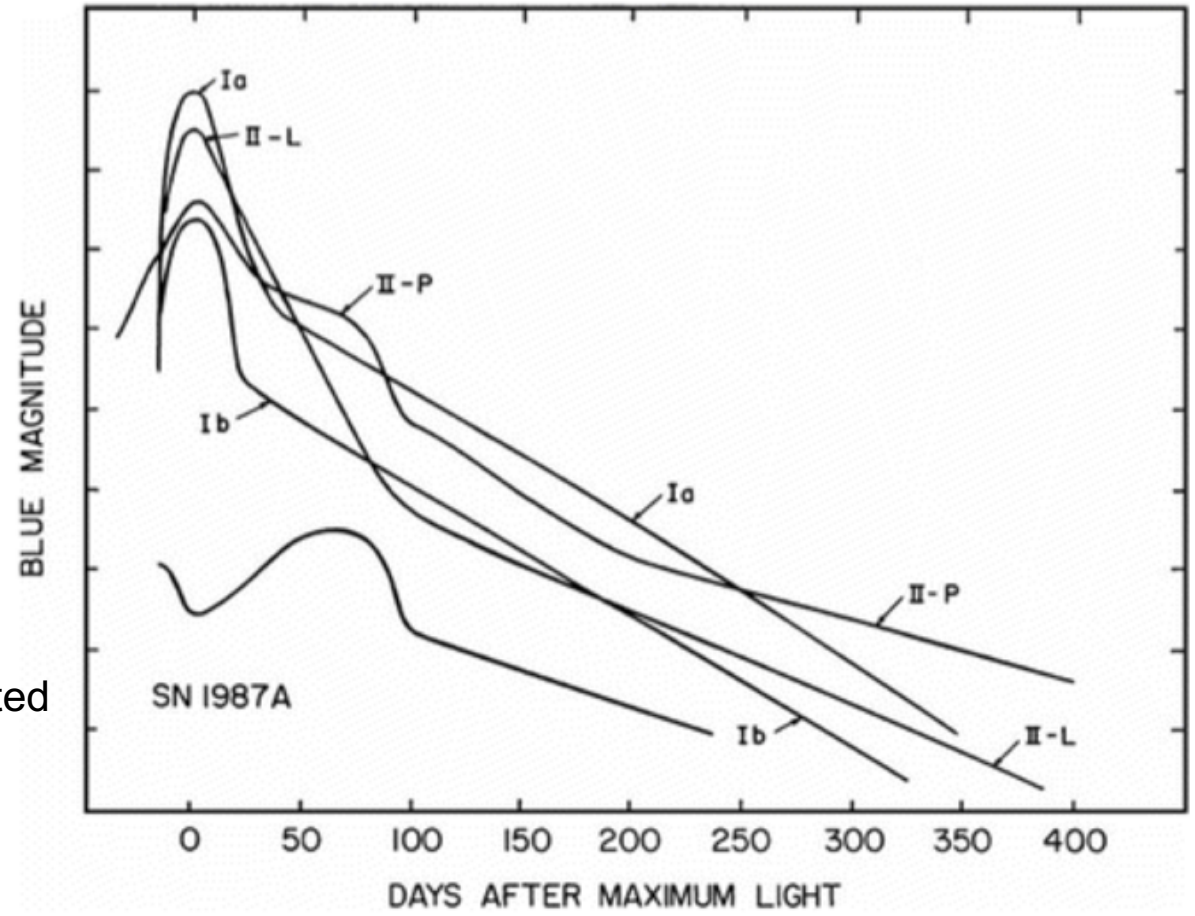

Fig. 1.5 A comparison of characteristic light curves. From "Introduction to Supernovae" (Wheeler 1990)

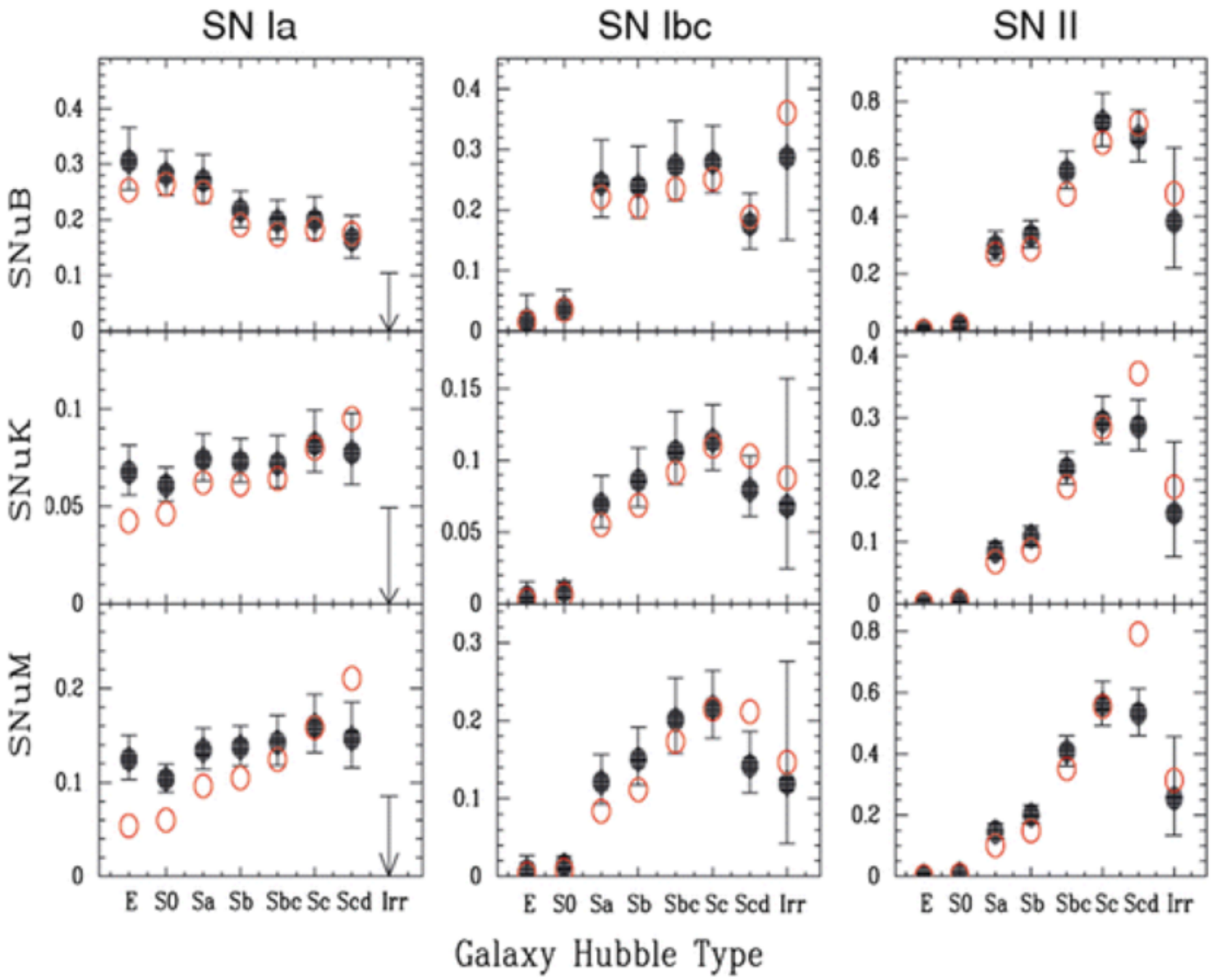

1 SNu = 1 supernova per 10^{10} (blue) solar luminosities per century

Properties: Type II supernovae

- Have strong Balmer lines – H_α, H_β, H_γ - in peak light and late time spectra. Also show lines of Fe II, Na I, Ca II, and, if the supernova is discovered early enough, He I.

- Clearly come from massive stars. Found in star forming regions of spiral and irregular galaxies. Not found in ellipticals. Several dozen presupernova stars have been identified: SN 1987A = B3 supergiant; SN 1993J = G8 supergiant (Aldering et al 1994)

- Usually fainter than Type Ia, but highly variable in brightness (presumably depending on hydrogen envelope mass and radius and the explosion energy). Typically lower speed than Type Ia. Last longer.

- Come in at least two varieties (in addition to 87A) – Type II-p or "plateau" and Type II-L or "linear". There may also be Type II-b supernovae which have only a trace amount of hydrogen left on what would otherwise have been a Type Ib/c (e.g., SN 1993J)

- Strong radio sources, and at least occasionally emit neutrino bursts

Typical Type II-p on the Plateau

Filippenko (1990)

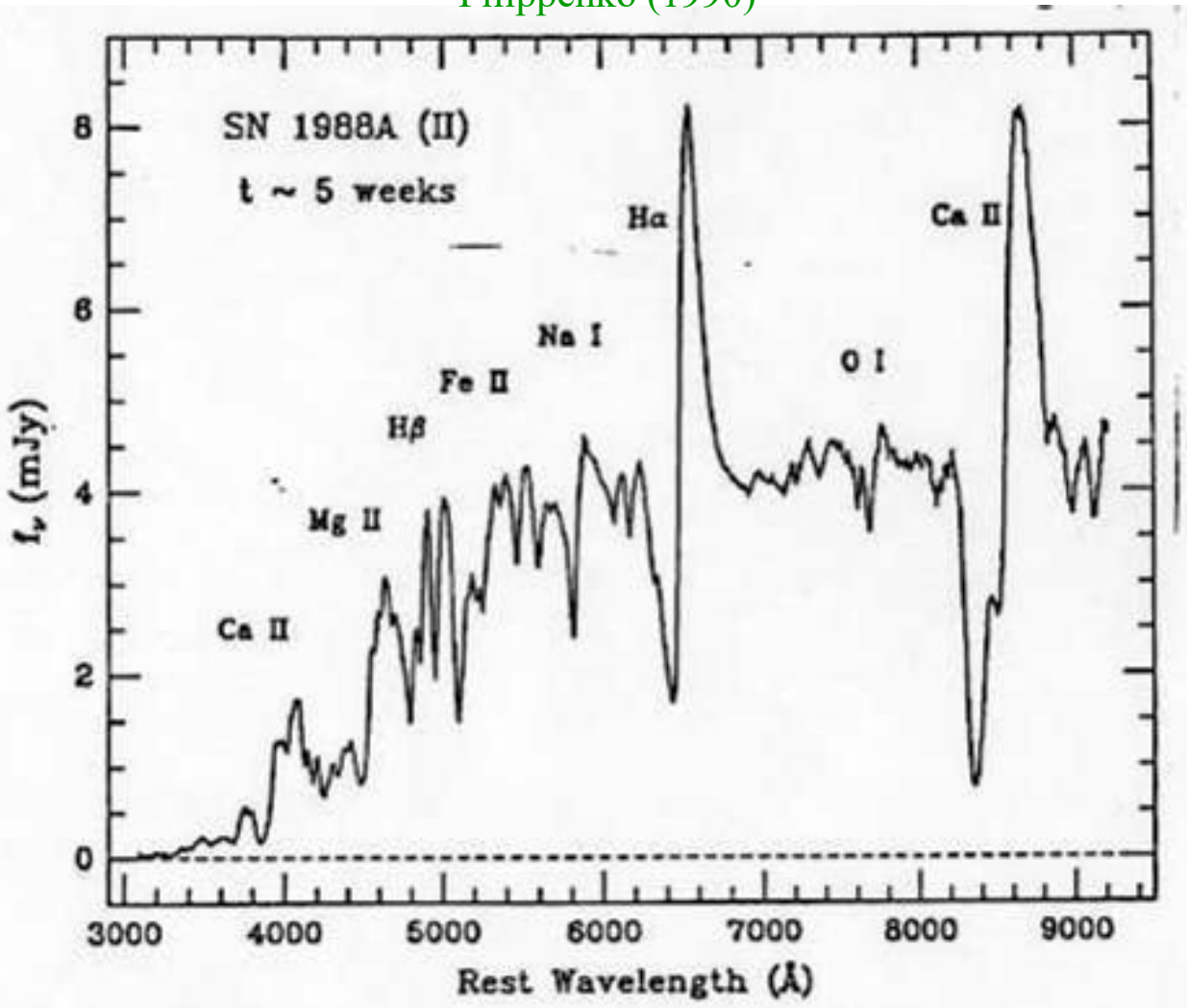

Figure 1: SN 1988A in M58, a typical SN II about 5 weeks past maximum brightness. Note the prominent P Cygni profiles, especially of Hα and the Ca II near-infrared triplet.

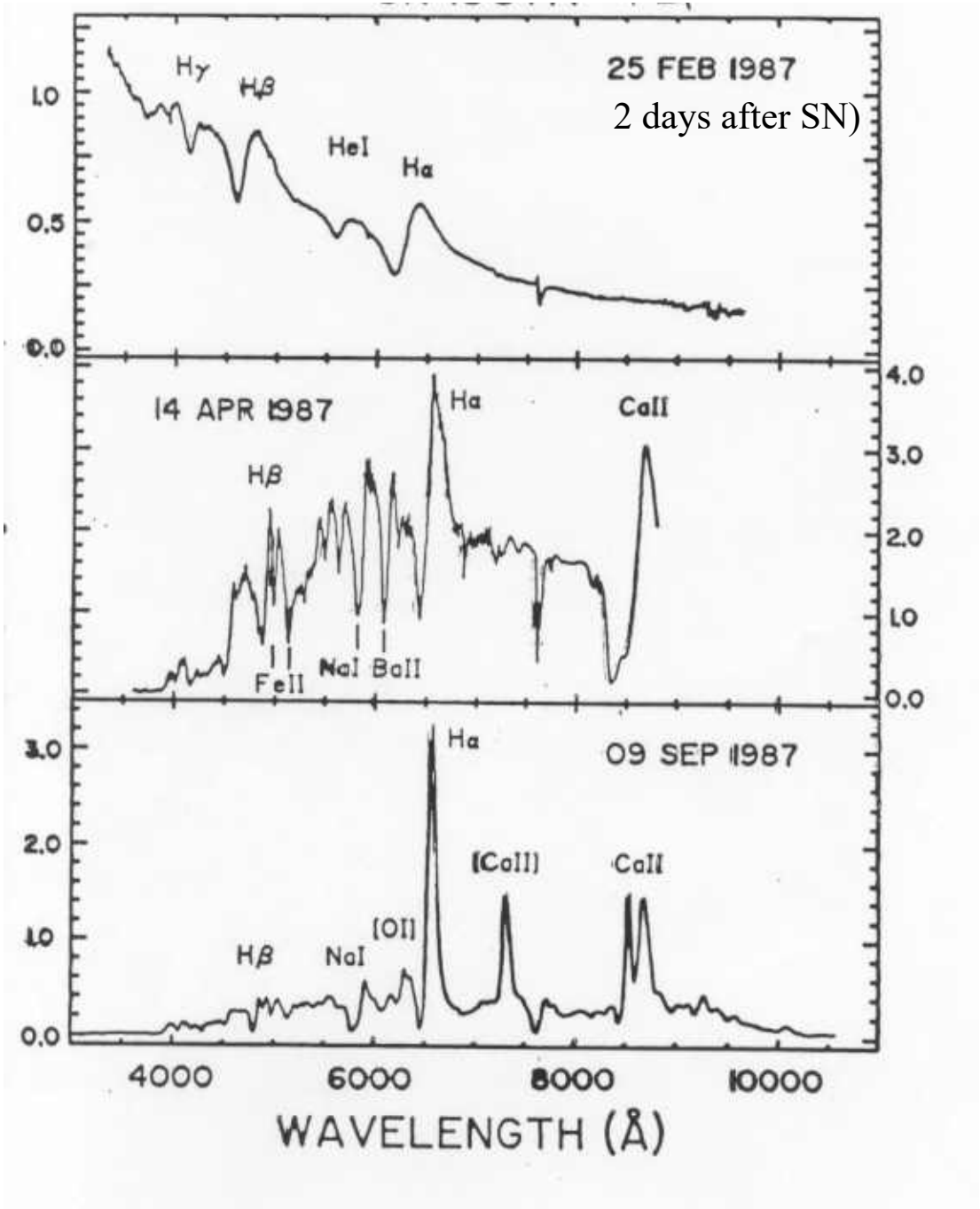

SN 1987A
Philipps (1987)
CTIO

Observational Properties: Type Ia supernovae

- The “classical” SN I; no hydrogen; strong Si II 6347, 6371 line
- Maximum light spectrum dominated by P-Cygni features of Si II, S II, Ca II, O I, Fe II and Fe III
- Nebular spectrum at late times dominated by Fe II, III, Co II, III
- Found in all kinds of galaxies, elliptical to spiral, some mild evidence for a association with spiral arms
- Prototypes 1972E (Kirshner and Kwan 1974) and SN 1981B (Branch et al 1981)
- Brightest kind of common supernova, though briefer. Higher average velocities. $M_{bol} \sim -19.3$
- Assumed due to an old stellar population. Favored theoretical model is an accreting CO white dwarf that ignites a thermonuclear runaway and is completely disrupted.

Spectra of SN Ia near maximum are very similar from event to event

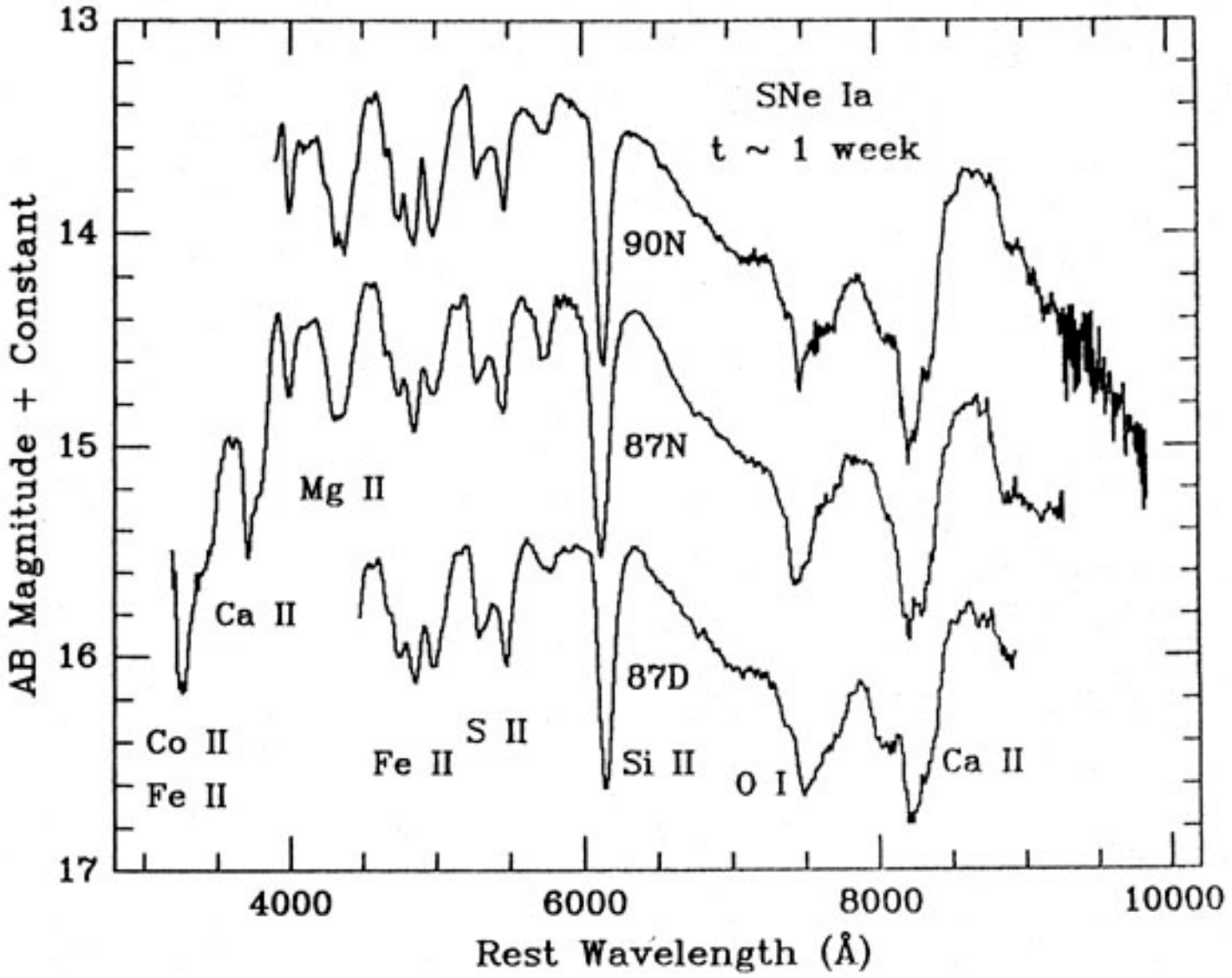

Spectra of three Type Ia supernovae near peak light – courtesy Alex Filippenko

Possible Type Ia Supernovae in Our Galaxy

	SN	D(kpc)	m_V
	185	1.2+-0.2	-8+-2
	1006	1.4+-0.3	-9+-1
Tycho	1572	2.5+-0.5	-4.0+-0.3
Kepler	1604	4.2+-0.8	-4.3+-0.3

Expected rate in the Milky Way Galaxy about 1 every 200 years, but dozens are found in other galaxies every year. About one SN Ia occurs per decade closer than about 5 Mpc.

2011fe a SN Ia reached apparent magnitude 9.9, 21 Mly. 72e was closer

Properties: Type Ib/c supernovae

- Lack hydrogen, but also lack the Si II $\lambda\lambda$6355 feature that typifies SN Ia.

- SN Ib have strong features due to He I at 5876, 6678, 7065 and 10830 A. SN Ic lack these helium features, at least the 5876 A line. Some people think there is a continuum of properties between SN Ib and SN Ic

- Found in spiral and irregular galaxies. Found in spiral arms and star forming regions. Not found in ellipticals. Associated with star formation

- Often strong radio sources (unlike Type Ia). Suggests extensive mass loss.

- Fainter at peak than SN Ia by about 1.5 magnitudes. Otherwise similar light curve.

- Only supernovae definitely associated with gamma-ray bursts so far are Type Ic

- Cannot have high mass in the common case. Probably come from binaries

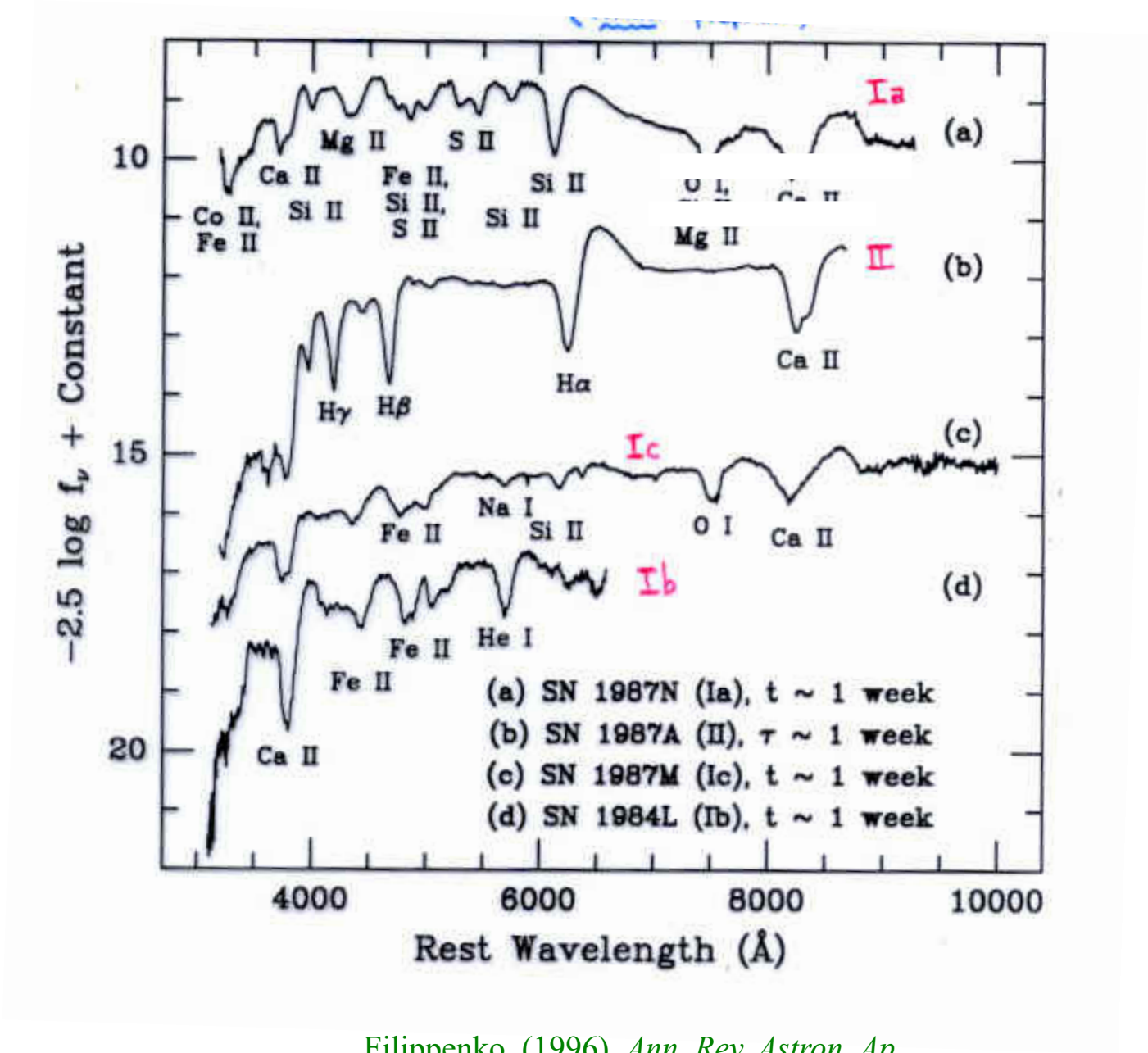

Filippenko, (1996), *Ann. Rev. Astron. Ap*

Miller and Branch (1990)

Richardson et al (2002)

Surveys of SN Types

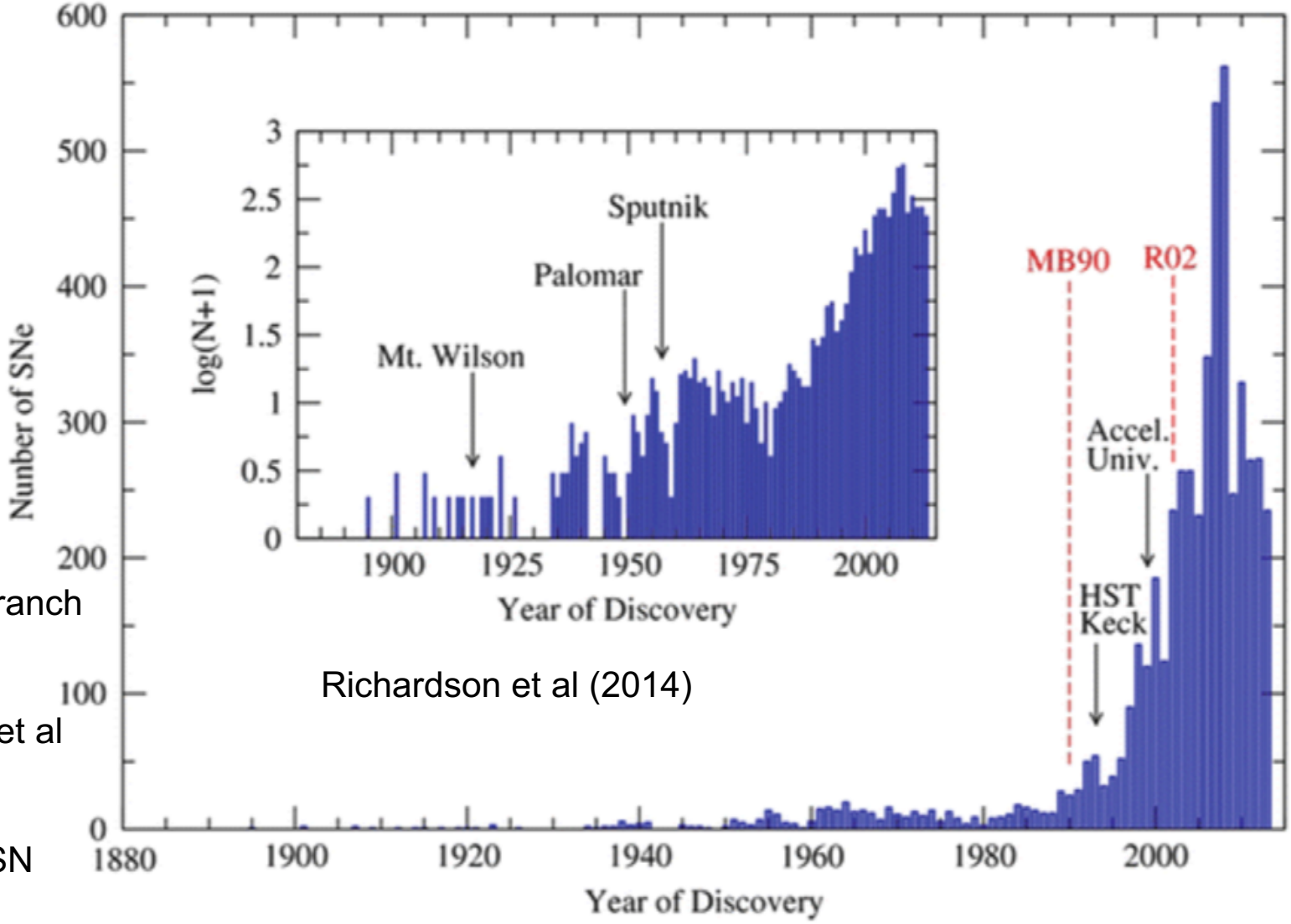

Richardson et al (2014)

1952 supernovae were discovered in 2014

7604 discovered in 2017

http://www.rochesterastronomy.org/sn2017/snstats.html

Supernova Discovery Future

Rough predictions and promises…

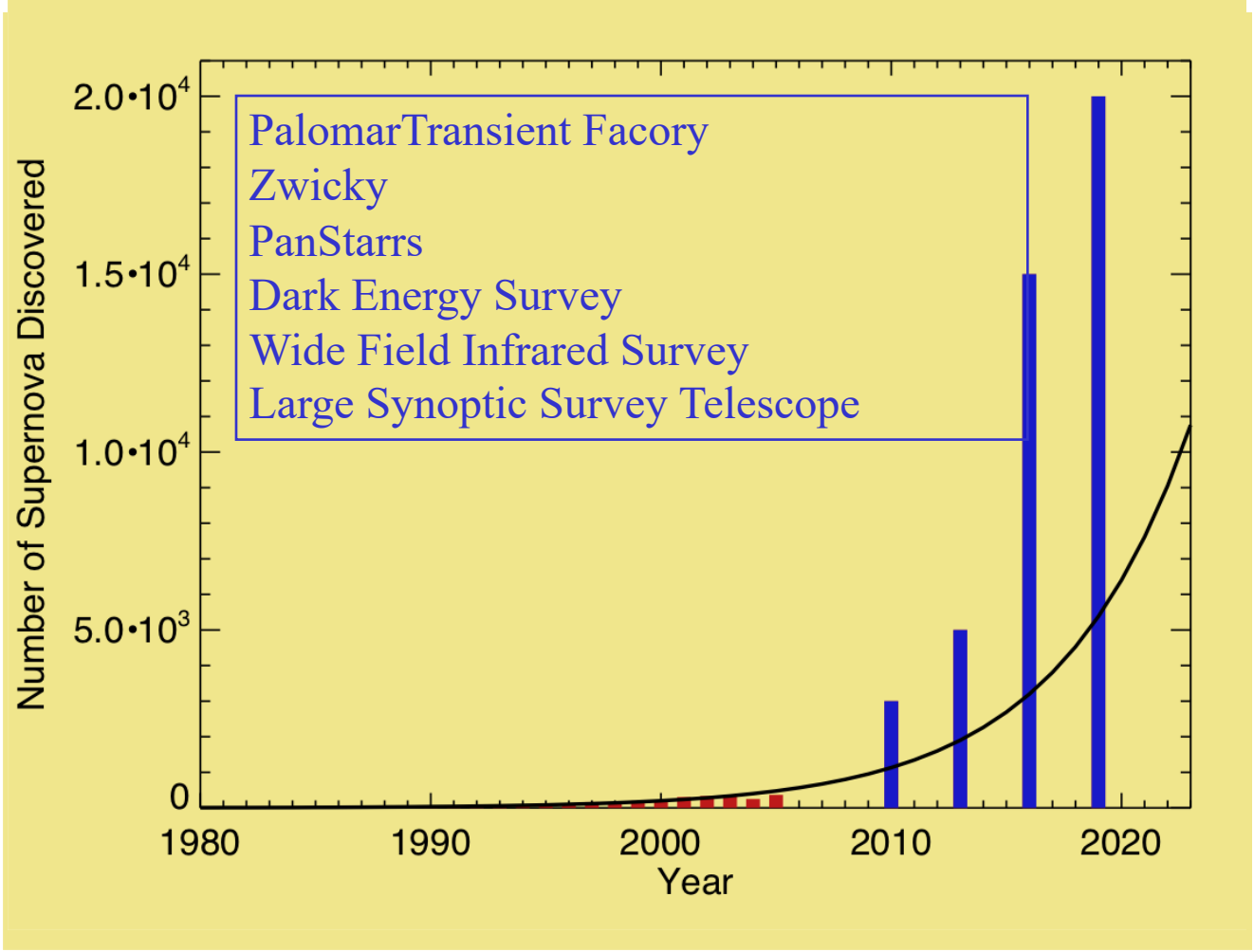

In a volume limited sample Li et al 2010, *MNRAS*, **412**, 1441

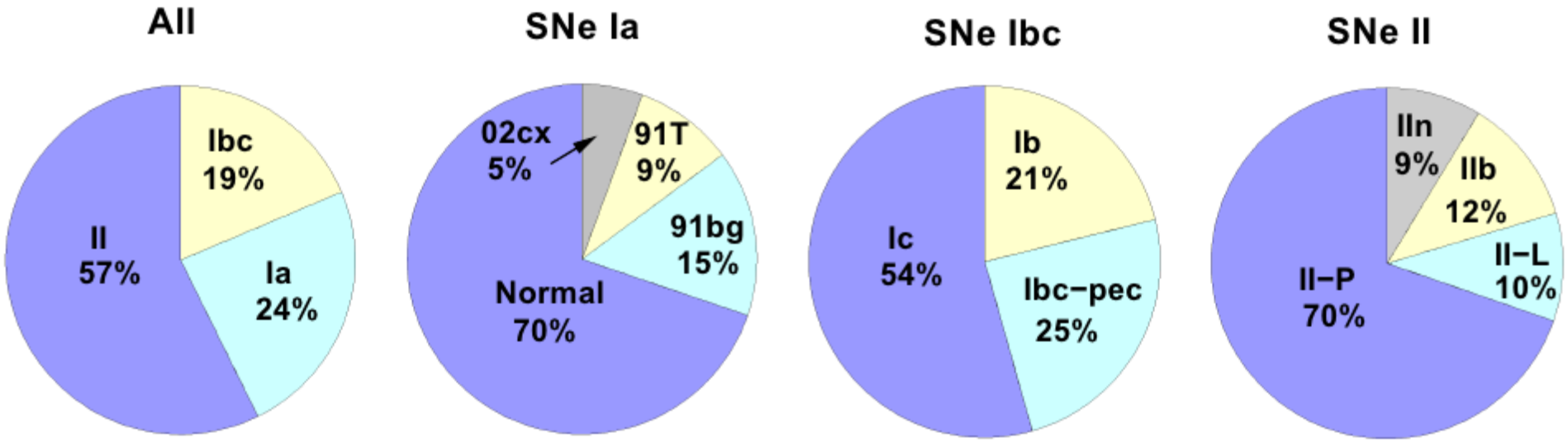

02cx is a class of very low luminosity SN Ia with slow speed and a non-nebular spectrum at late times

91T is a very bright type of Ia

91bg is also faint. Spectrum dominated by intermediate mass elements including Ti II. Also O I may be present.

Core collapse only

Table 1. The relative frequency of CCSN types discovered between 1998 and 2012.25 (14.25 yr) in galaxies with recessional velocities less than 2000 km s^{-1}, as listed in Table A1. The values in parentheses in the Number column include SNe of indeterminate subtype as discussed in the text.

SN Type	Number	Relative rate (per cent)	LOSS (per cent)
IIP	55 (70.5)	55.5 ± 6.6	$48.2\ ^{+5.7}_{-5.6}$
IIL	3 (3.8)	3.0 ± 1.5	$6.4\ ^{+2.9}_{-2.5}$
IIn	3 (3)	2.4 ± 1.4	$8.8\ ^{+3.3}_{-2.9}$
IIb	12 (15.4)	12.1 ± 3.0	$10.6\ ^{+3.6}_{-3.1}$
IIpec (87A-like)	1 (1.3)	1.0 ± 0.9	–
Ib	9 (11.4)	9.0 ± 2.7	$8.4\ ^{+3.1}_{-2.6}$
Ic	17 (21.6)	17.0 ± 3.7	$17.6\ ^{+4.2}_{-3.8}$
Total	100 (127)		

Eldridge et al (MNRAS 436 774 (2013))

Tammann et al (1994) says total SN
rate in MW is one every 40+-10 years, with 85% from massive stars.
The very largest spirals produce about 10 SNae per century.

Good rule of thumb - 2 core collapse supernovae per centery;
one SN Ia every other century

Type IIp Supernovae
Models and Physics of the Light Curve

- the most common kind of supernova

APPROXIMATIONS

Light curve peak for an expanding sphere with mass M filled with trapped radiation occurs when $\tau_{dif} = t$

$$\mathrm{t}_{peak} \approx \frac{R^2 \kappa \rho}{c} \approx \frac{R^2 \kappa (3M)}{c(4\pi R^3)} = \frac{3\kappa M}{4\pi c R}$$

but $R = vt \sim \left(\frac{2E}{M}\right)^{1/2} t$ so

$$\mathrm{t}_{peak} = \frac{3\kappa M}{4\pi c} \frac{M^{1/2}}{(2E)^{1/2} t_{peak}}$$

$$t_{peak} = \left(\frac{3\kappa M}{4\pi c}\right)^{1/2} \left(\frac{M}{2E}\right)^{1/4}$$

$$= 15 \text{ days} \left(\frac{\kappa}{0.1}\right)^{1/2} \left(\frac{M}{M_\odot}\right)^{3/4} \left(\frac{10^{51} \text{ erg}}{E}\right)^{1/4}$$

The radius then is

$$\mathrm{R} \approx \mathrm{vt}_{peak} = \left(\frac{2E}{M}\right)^{1/2} t_{peak} = 1.3 \times 10^{15} \text{ cm} \left(\frac{\kappa}{0.1}\right)^{1/2} \left(\frac{M}{M_\odot}\right)^{1/4} \left(\frac{10^{51} \text{ erg}}{E}\right)^{3/4}$$

APPROXIMATIONS

The luminosity is approximately the internal energy at that point divided by the diffusion time (or age)

$$\mathrm{L} \approx \frac{E(t_{peak})}{t_{peak}} = E_0 \left(\frac{R_0}{R} \right) t_{peak}^{-1} \qquad R t_{peak} = \frac{3\kappa M}{4\pi c}$$

since $\varepsilon \sim \frac{aT^4}{\rho}$ and radiation entropy $\frac{T^3}{\rho}$ is constant and $\rho \propto \frac{1}{R^3}$

$$L(t_{peak}) \approx E_0 R_0 \left(\frac{4\pi c}{3\kappa M} \right)$$

$$= 6 \times 10^{42} \text{ erg s}^{-1} \left(\frac{E_0}{10^{51}} \right) \left(\frac{R_0}{10^{13}} \right) \left(\frac{0.1}{\kappa} \right) \left(\frac{M_\odot}{M} \right)$$

Note: For R ~ 10^{15} cm will emit chiefly in the optical
Brighter for larger initial radius and explosion energy
Brighter for smaller opacity and smaller mass (provided $E_0 = 10^{51}$ erg).
Will peak earlier for lower masses

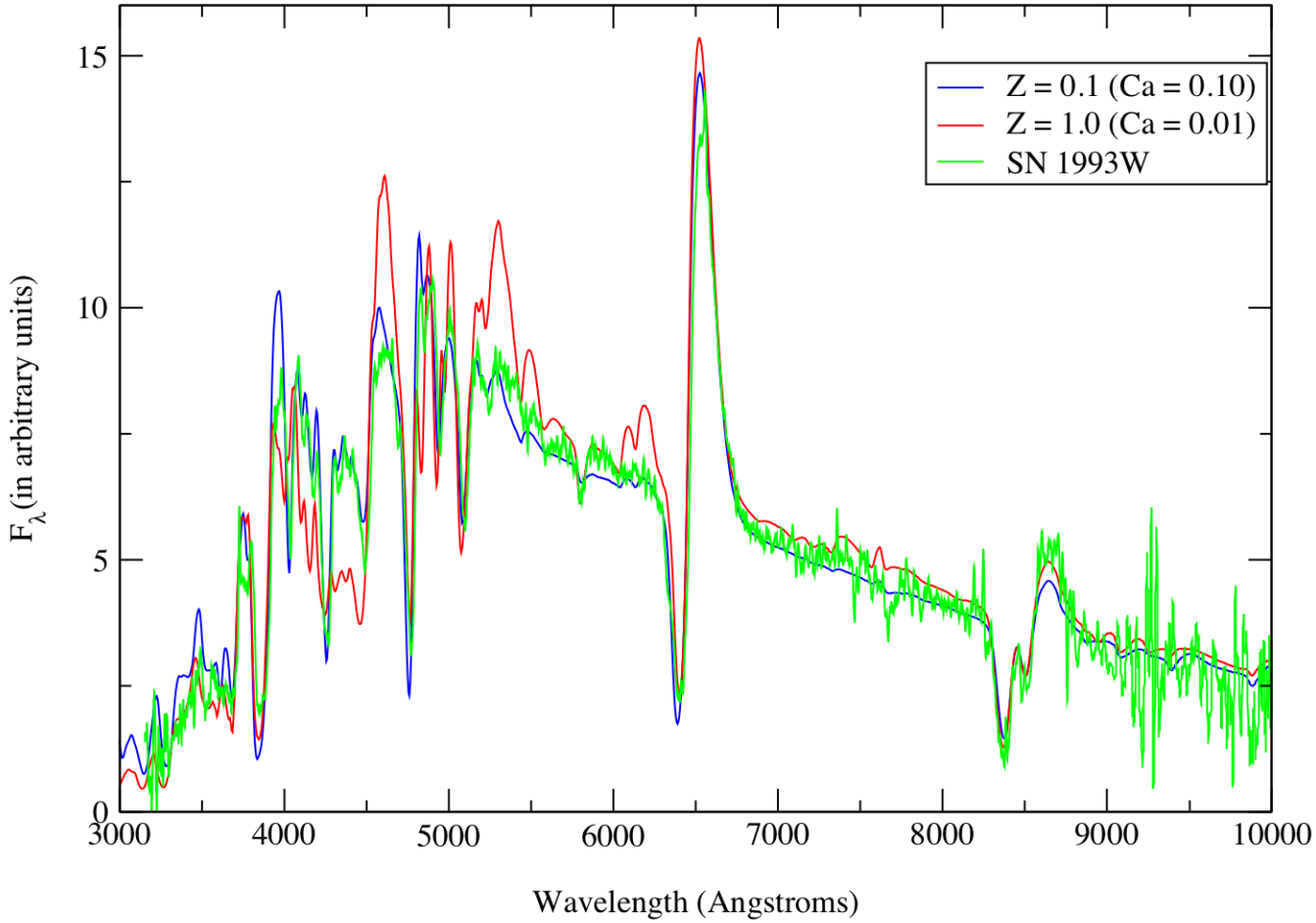

Modeling the spectrum of a Type II supernova in the Hubble flow (5400 km/s) by Baron et al. (2003). SN 1993W at 28 days. The spectrum suggests low metallicity.

KASEN & WOOSLEY (2009)

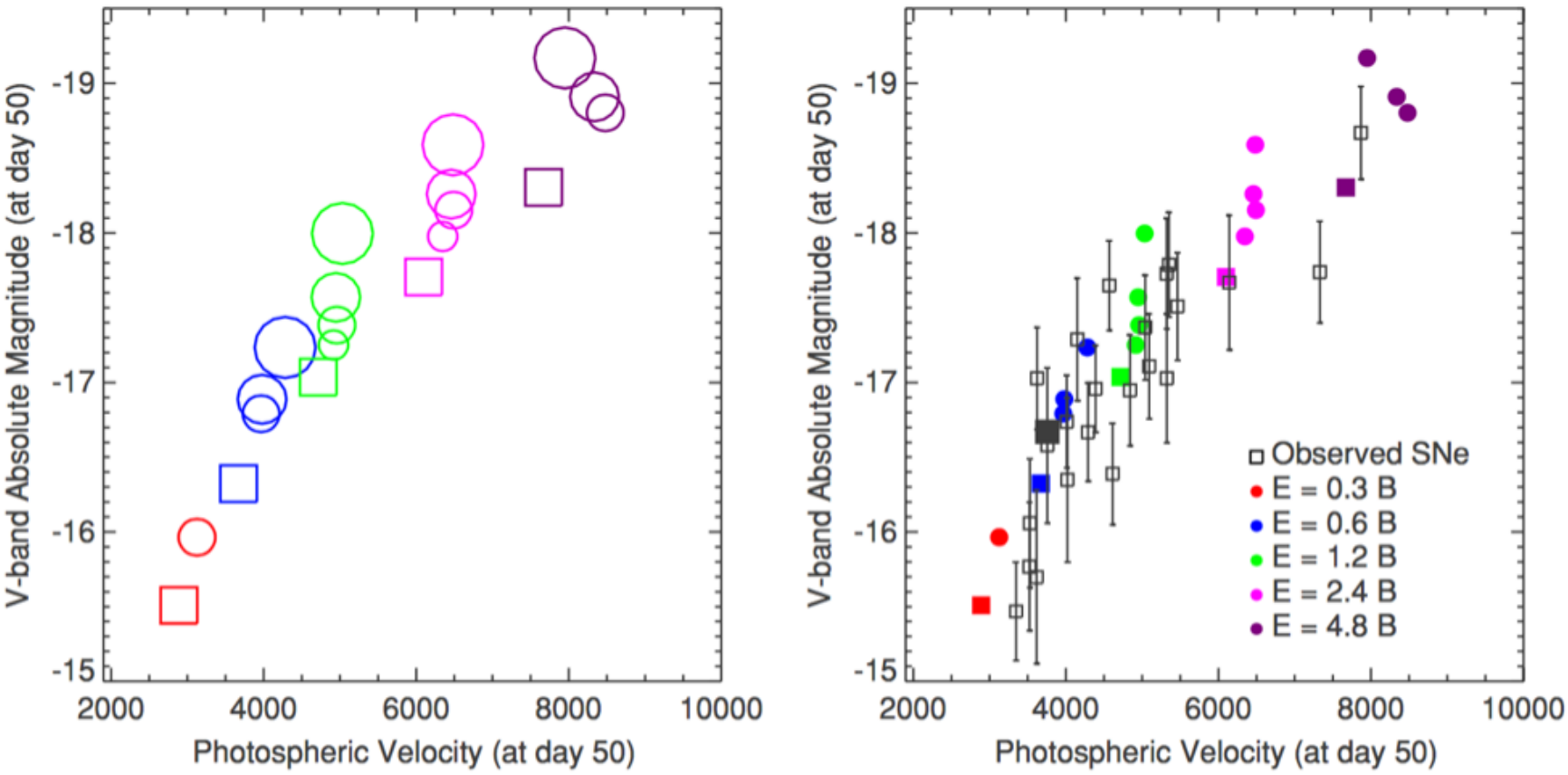

Common SN IIp have a range of explosion energies from ~0.5 to 4 x 10^{51} with an average of 0.9 x 10^{51} erg. Magnitude on the plateau is correlated with explosion velocity. The colored points are numerical models

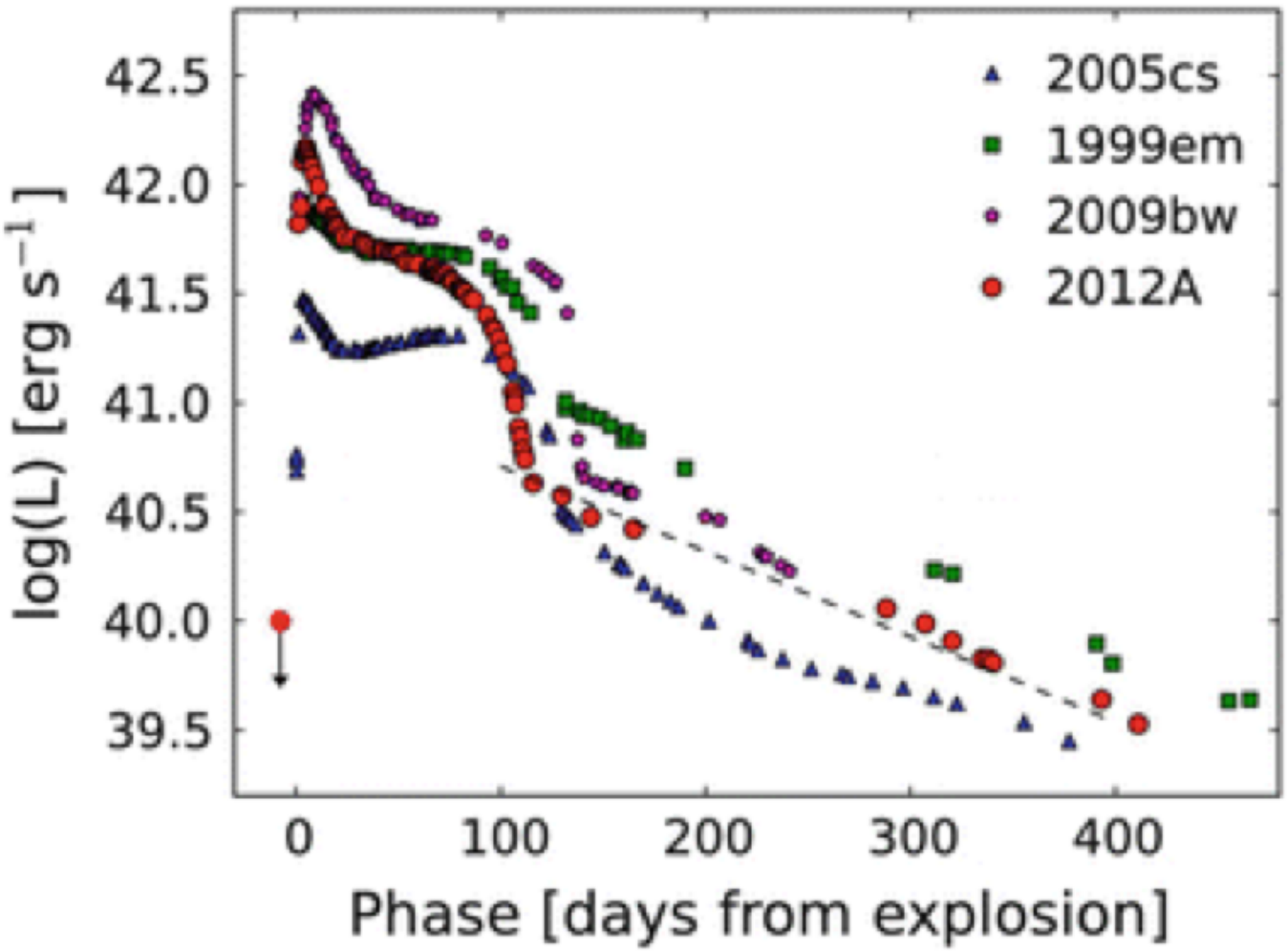

Tomasella et al (2013)

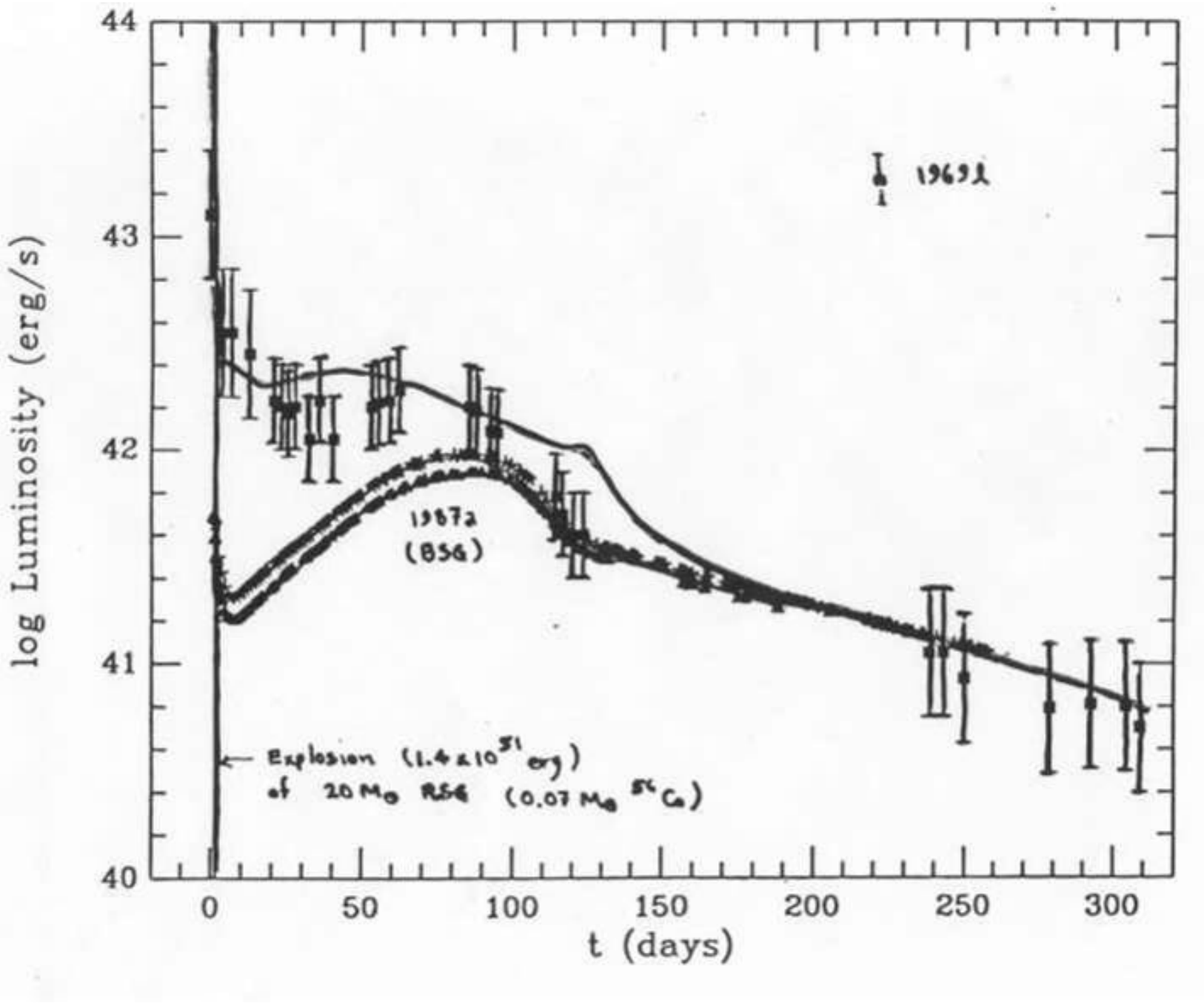
log Luminosity (erg/s)
44
43
42
41
40
0
50
100
150
200
250
300
t (days)
1969L
1987A
(BSG)
← Explosion (1.4 x 10^51 erg)
of 20 M⊙ RSG (0.07 M⊙ 56Co)

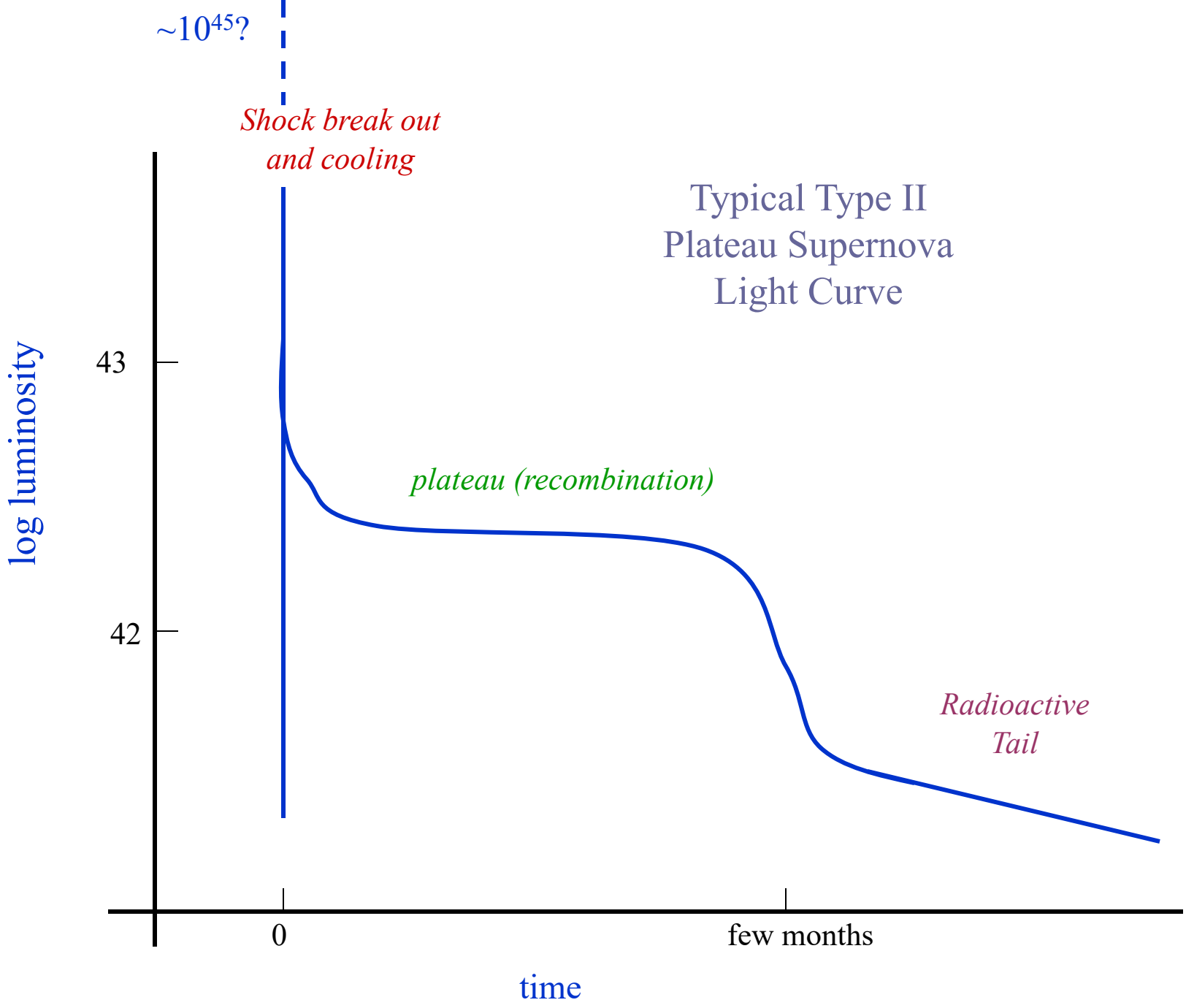
~10^45?
Shock break out
and cooling
Typical Type II
Plateau Supernova
Light Curve
log luminosity
43
42
plateau (recombination)
Radioactive
Tail
0
few months
time

For a typical red supergiant derived from a star over 8 solar masses.

- *Break out – temperatures of 100's of thousands K. Very brief stage, not observed so far (indirectly in 87A). Shock heating followed by expansion and cooling*

- *Plateau – the hydrogen envelope expands and cools to ~5500 K. Radiation left by the shock is released. Nearly constant luminosity (T is constant and radius of photosphere does not change much – around 10^{15} cm). Lasts until the entire envelope recombines.*

- *Radioactive tail – powered by the decay of radioactive ^{56}Co produced in the explosion as ^{56}Ni.*

The light curve will vary depending upon the mass of the envelope, radius of the presupernova star, energy of the explosion, degree of mixing, and mass of ^{56}Ni produced.

Shock Break-out

The electromagnetic display begins as the shock wave erupts through the surface of the star. A brief, hard ultra-violet (or even soft x-ray) transient ensues as radiation diffuses from behind the erupting shock The transient is brighter and longer for larger progenitors but hotter for smaller ones

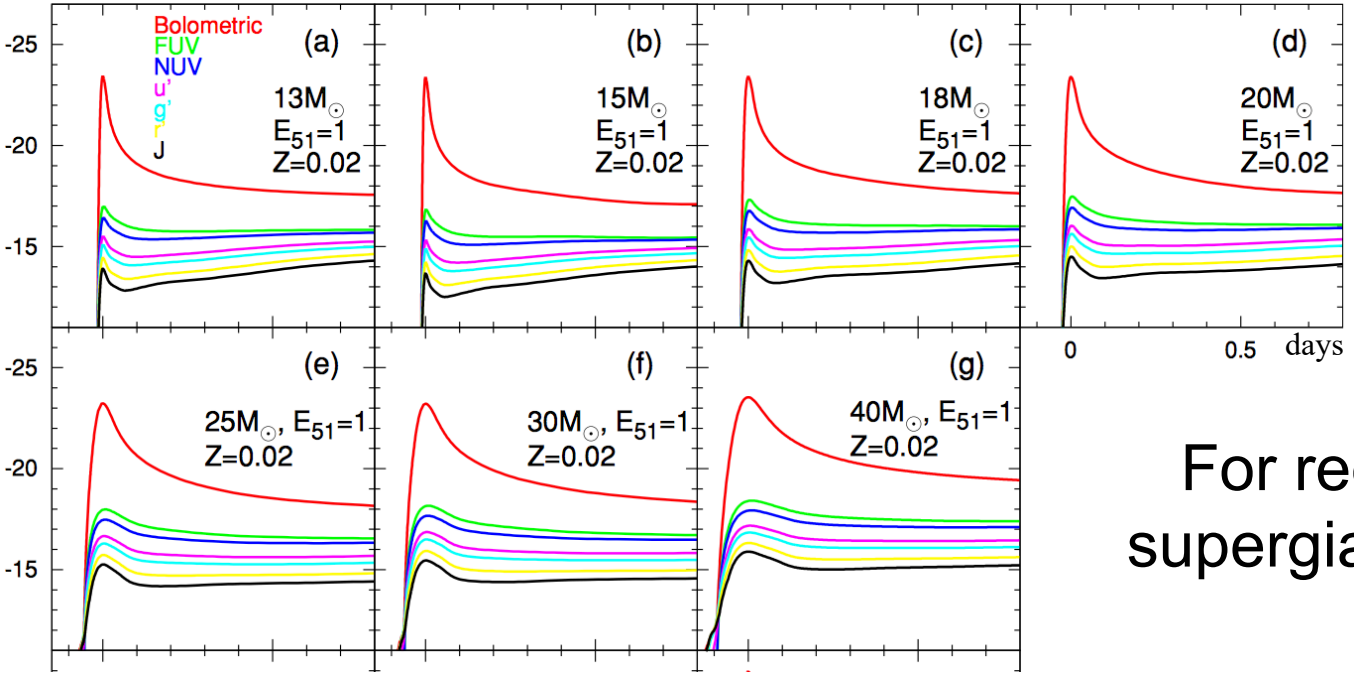

For red supergiants

Tominaga et al. 2011, *ApJ*, **193**, 20

Shock breakout commences when the diffusion time through the matter outside the shock equals the shock crossing time for the same region

$$\frac{(\Delta r)^2 \kappa\rho}{c} \approx \frac{\Delta r}{v_s}$$

and $\kappa\rho\Delta r = \tau = \frac{c}{v_s} \sim 20$

The number of scatterings, $\sim\tau^2$, is generally inadequate to thermalize the escaping photons, hence $T_{color} > T_{eff}$

The duration is set by a) the shock crossing time for τ=20 or about 0.01 $R/v_s \sim .01 \bullet 6\times10^{13} / 2\times10^{9} = 300$ s for a red supergiant (a minimum) b) the diffusion time out of the shock heated layer (which is deeper than τ=20); c) the expansion time for that layer perhaps 0.1 R/v_s = 3000 s; d) the light crossing time for the star R/c ~ 2000 s (R/6 $\times10^{13}$)

Piro (2013) gives for cases where diffusion dominates

$$L_{bo} = 1.7\times10^{45}\ \mathrm{erg\ s^{-1}}\ \frac{E_{51}^{1.36}}{\kappa_{.34}^{.29} M_{10}^{.65} R_{1000}^{0.42}}\left(\frac{\rho_1}{\rho_*}\right)^{0.194}$$

where ρ_1 / ρ_* is about 0.5 (Calzavara and Matzner 2004)

The temperature is

$$T = 1.5\times10^{5}\ K\ \frac{E_{51}^{0.34}}{\kappa_{.34}^{.068} M_{10}^{.16} R_{1000}^{0.61}}\left(\frac{\rho_1}{\rho_*}\right)^{0.049}$$

where M_{10} is the mass of the envelope in 10 $M_\odot$ units and

R_{1000} is the radius in units of 1000 $R_\odot$, i.e. 6.9×10^{13} cm

Note that for more compact stars the breakout will be fainter and hotter. κ is generally due to electron scattering until the energy becomes very low.

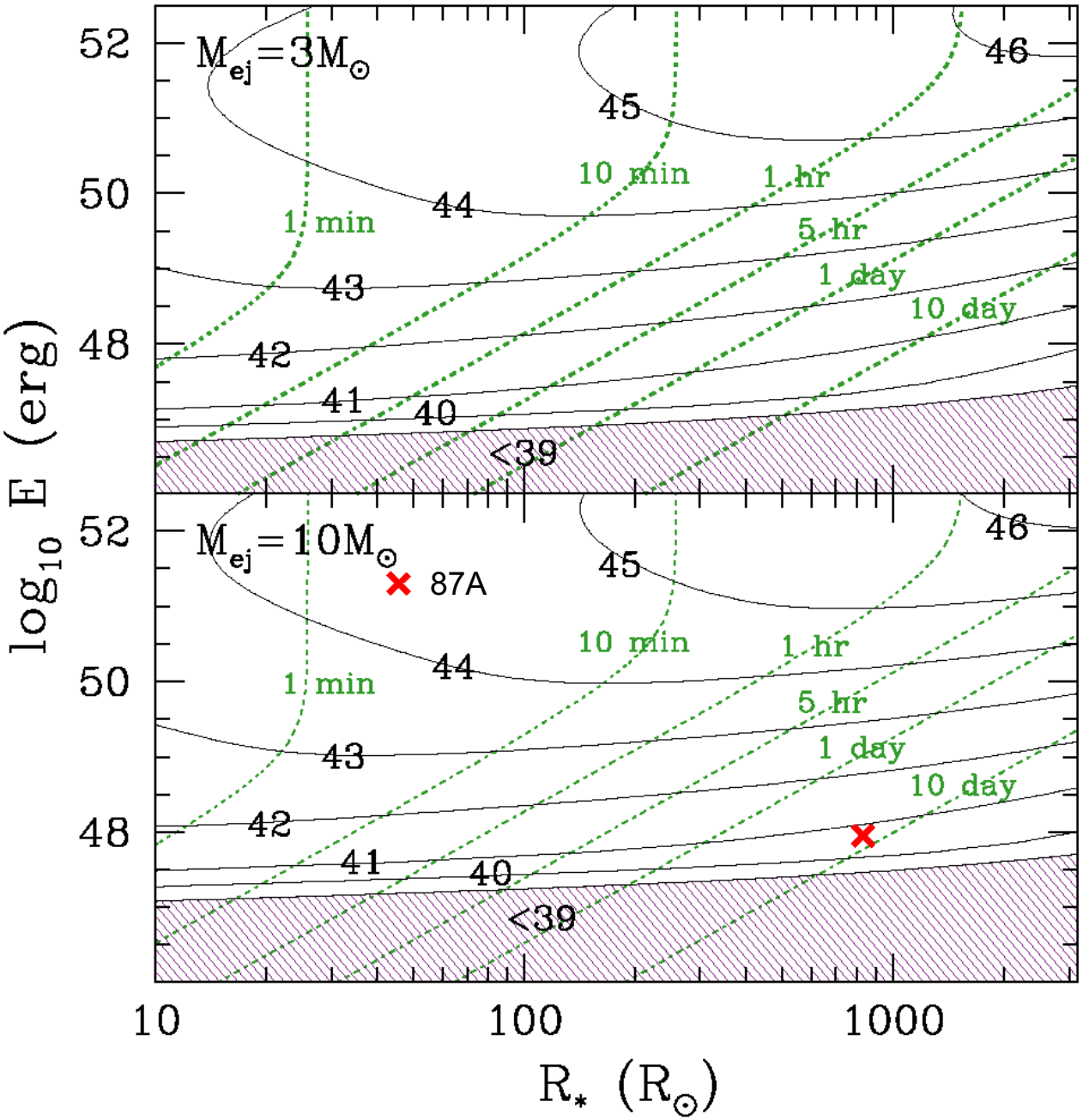
$M_{ej}=3M_\odot$
$M_{ej}=10M_\odot$
87A
46
45
44
43
42
41
40
<39
1 min
10 min
1 hr
5 hr
1 day
10 day
52
50
48
$\log_{10}$ E (erg)
10
100
1000
R_* ($R_\odot$)

Table 2
Properties of Shock Breakout

M_{MS} ($M_\odot$)	Z	E (10^{51} erg)	M_{ej} ($M_\odot$)	$T_{c,peak}$ (10^5 K)	$t_{1\,mag}$ (10^{-2} days)	$E_{rad,1\,mag}$ (10^{48} erg)	L_{peak} (10^{44}erg s^{-1})	$T_{c,peak}$ (10^5 K)	$t_{1\,mag}$ (10^{-2} days)	$E_{rad,1\,mag}$ (10^{48} erg)	L_{peak} (10^{44}erg s^{-1})
					Without Corrections				With Corrections		
13	0.02	1	11.2	3.56	0.651	0.691	10.3	3.35	1.09	0.815	6.99
15	0.02	1	12.7	3.68	0.512	0.536	10.2	3.48	0.915	0.643	6.64
18	0.02	1	15.2	3.03	0.994	0.948	9.41	2.87	1.46	1.09	6.90
20	0.02	1	16.8	2.80	1.19	1.11	9.11	2.70	1.68	1.26	6.91
25	0.02	1	19.9	2.17	2.94	2.07	6.78	2.04	3.40	2.23	5.99
30	0.02	1	23.0	1.99	3.51	2.39	6.52	1.87	3.97	2.54	5.86
40	0.02	1	19.6	2.01	5.16	4.57	8.55	1.92	5.60	4.82	7.90
25	0.02	4	19.8	3.23	1.27	4.20	32.5	3.08	2.28	5.05	21.1
25	0.02	10	19.7	4.38	0.763	6.83	89.6	3.96	2.12	8.74	42.4
25	0.02	20	19.6	5.21	0.511	10.0	196	4.88	2.06	13.5	72.4
20	0.001	1	17.9	2.57	1.35	0.896	6.51	2.51	1.77	1.01	5.23
20	0.004	1	17.8	2.91	1.09	0.986	8.80	2.76	1.54	1.12	6.64
20	0.05	1	15.7	2.41	2.14	1.80	8.09	2.31	2.64	1.99	6.88

Tominaga et al. 2011, *ApJ*, **193**, 20

0.01 d = 864 s

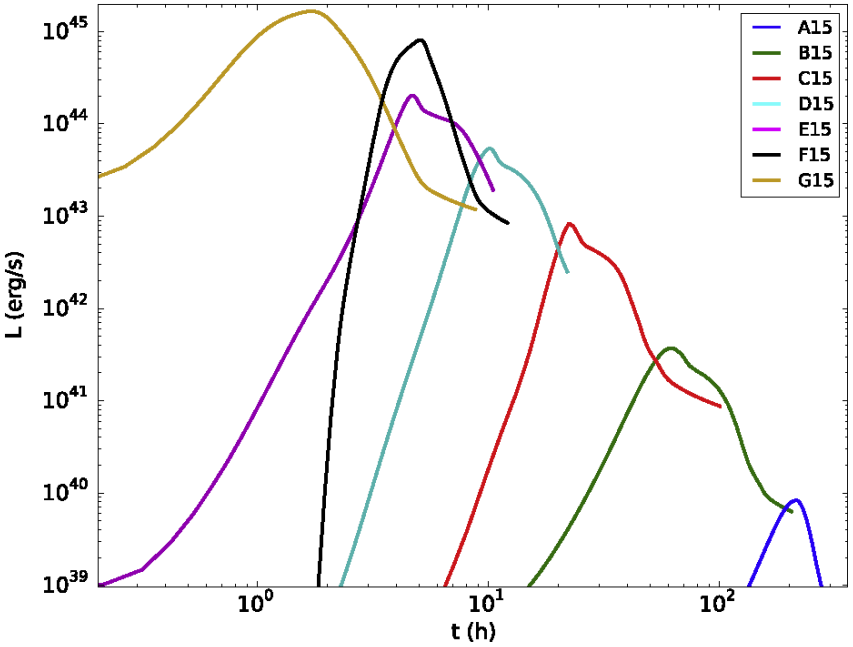

Figure 13. Bolometric light curves for RSG15 shock breakouts at seven different final kinetic energies ranging from 6.58×10^{46} (A15) to 1.20×10^{51} (G15), calculated by CASTRO. Both peak luminosity and breakout flash duration show clear and significant variations with explosion

Lovegrove et al (2017)

Table 4
Comparison to Other Models

Model	KE_f[a] (erg)	L_{peak} (erg s^{-1})	L_K[b] (erg s^{-1})	Pred. L (erg s^{-1})	Max T_{ef} (K)	$T_{ef,k}$[c](K)	Pred. T_{ef} (K)
A15	6.58×10^{46}	9.50×10^{39}	5.09×10^{39}	4.25×10^{39}	8.15×10^{3}	6.93×10^{3}	6.29×10^{3}
B15	1.54×10^{48}	3.89×10^{41}	3.94×10^{41}	3.10×10^{41}	2.06×10^{4}	1.99×10^{4}	1.84×10^{4}
C15	1.21×10^{49}	8.31×10^{42}	6.32×10^{42}	5.11×10^{42}	4.44×10^{4}	4.02×10^{4}	3.71×10^{4}
D15	5.04×10^{49}	5.43×10^{43}	3.95×10^{43}	3.56×10^{43}	7.08×10^{4}	6.36×10^{4}	6.02×10^{4}
E15	1.23×10^{50}	2.13×10^{44}	1.17×10^{44}	1.20×10^{44}	9.97×10^{4}	8.34×10^{4}	8.15×10^{4}
F15	5.07×10^{50}	8.25×10^{44}	6.17×10^{44}	8.06×10^{44}	1.40×10^{5}	1.30×10^{5}	1.31×10^{5}
G15	1.20×10^{51}	1.68×10^{45}	1.76×10^{45}	2.65×10^{45}	1.67×10^{5}	1.69×10^{5}	1.77×10^{5}

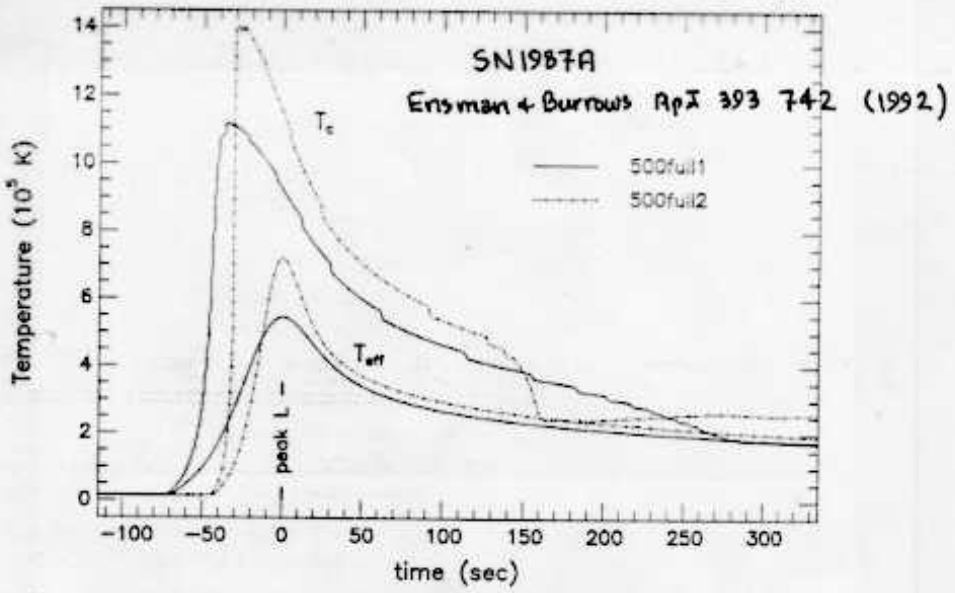

FIG. 11.—Color temperature and effective temperature of the emitted radiation as a function of time since peak luminosity for models 500full1 and 500full2. The top curve for each model is the color temperature, which is equal to the radiation temperature (and the gas temperature, except when the shock front passes through) at the thermalization depth. The small steps in the curves are numerical artifacts.

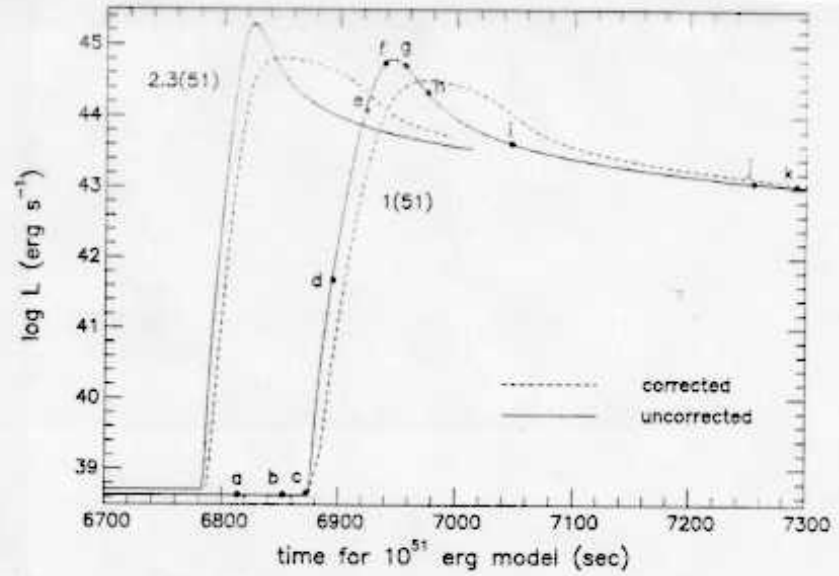

For SN 1987A detailed calculations exist. It was little hotter, briefer and fainter because it was a BSG with 10 times smaller radius than a RSG.

The effect of the uv-transient in SN 1987A was observed in the circumstellar ionization that it caused. The first spectroscopic observations of SN 1987A, made 35 hours after core collapse (t = 0 defined by the neutrino burst) – Kirshner et al, *ApJ*, **320**, 602, (1987), showed an emission temperature of 15,000 K that was already declining rapidly.

Ultraviolet observations later (Fransson et al, ApJ, 336, 429 (1989) showed *narrow* emission lines of N III, N IV, N V, and C III (all in the 1200 – 2000 Angstrom band). The ionization threshold for these species is 30 to 80 keV.

Modeling (Fransson and Lundquist *ApJL*, **341**, L59, (1989)) implied an irradiating flux with $T_e = 4$ to 8×10^5 K and an ionizing fluence (> 100 eV) ~ 2×10^{46} erg. This is in good agreement with the models.

The emission came from a circumstellar shell around the supernova that was ejected prior to the explosion – hence the narrow lines.

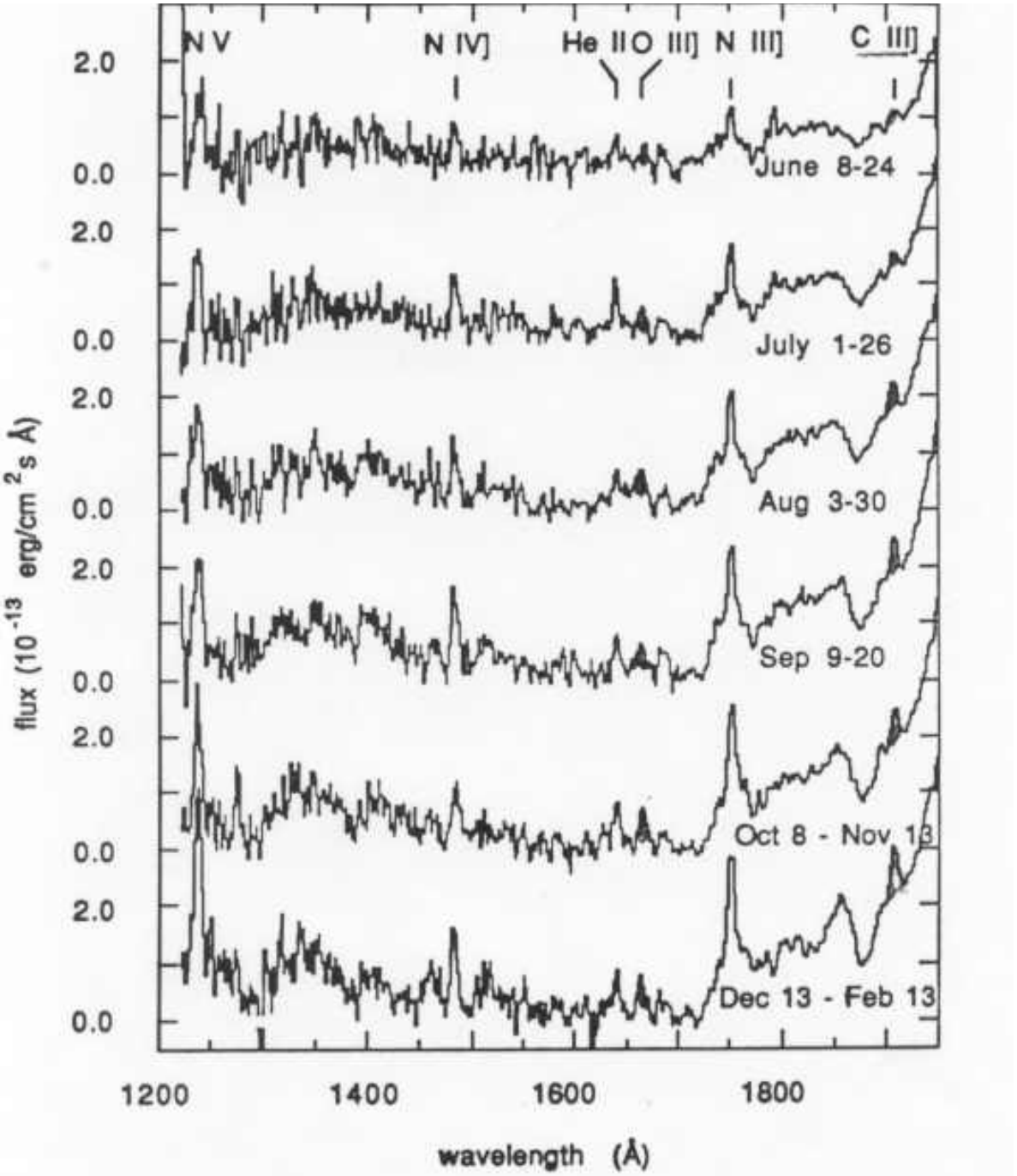

Fransson et al (1989)

IUE Observations of circumstellar material in SN 1987 A

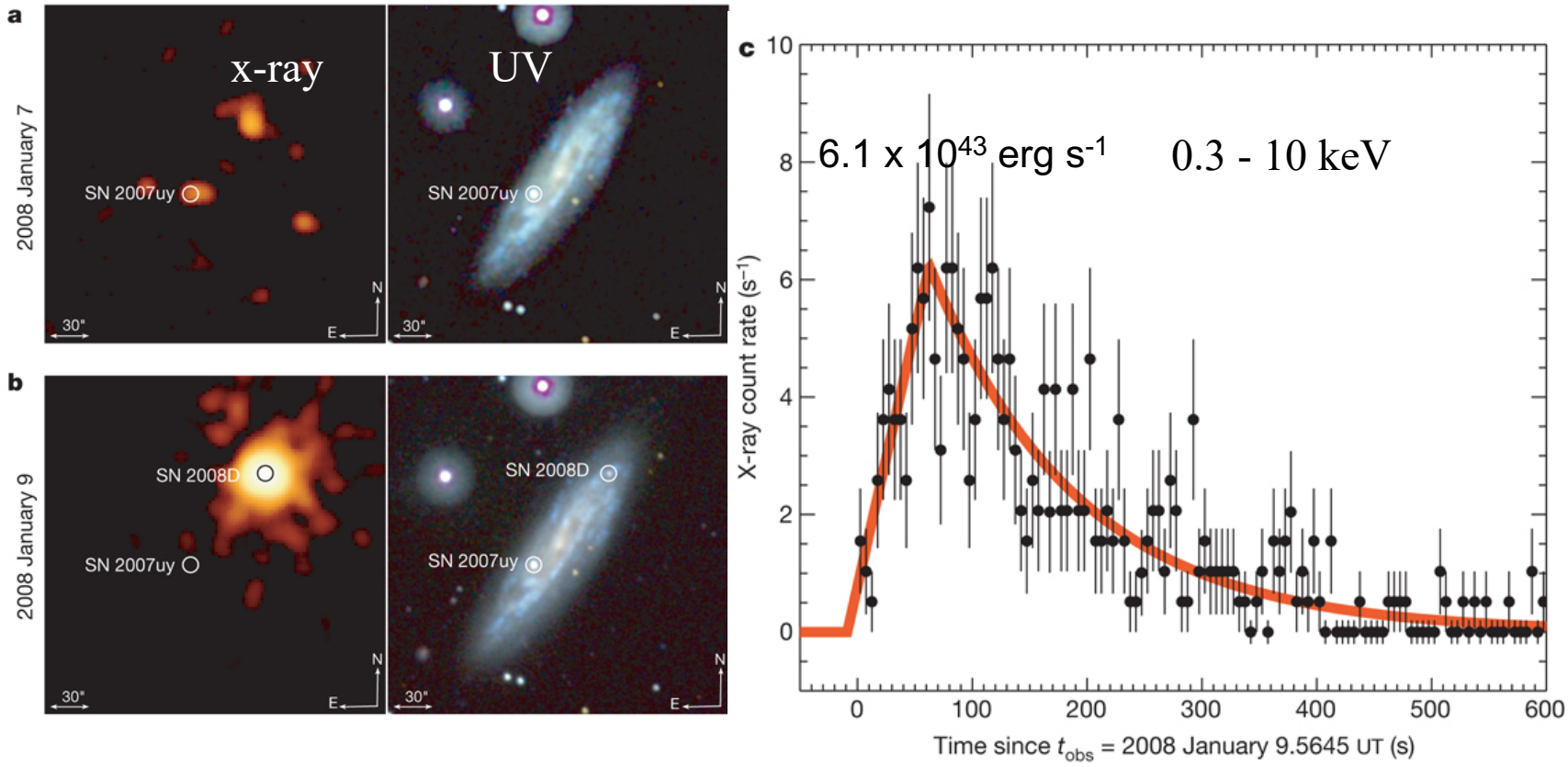

Soderberg et al 2008, *Nature*, **453**, 469

Shock breakout in Type Ib supernova SN 2008D
(serendipitous discovery while observing SN 2007uy)

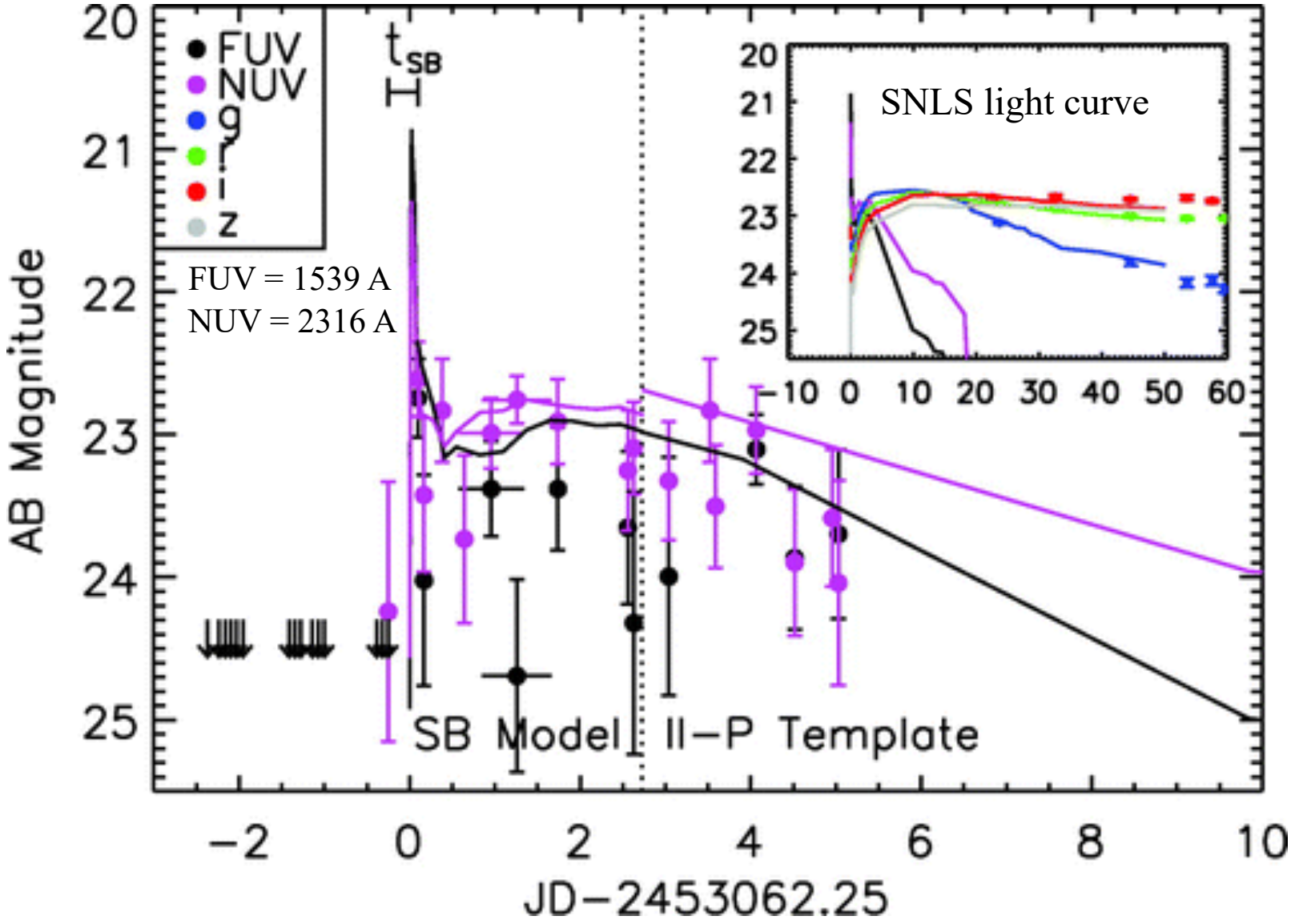

GALLEX discovery of ultraviolet emission just after shock break-out in a Type II-p supernova (Gezari et al 2008, ApJ, 683, L131). Missed the initial peak (about 2000 s, 90 Angstroms) but captured the 2 day uv-plateau

Modeling shows that they captured two supernovae, SNLS-04D2dc and SNLS-06D1jd within 7.1 hr and 13.7 hr after shock break out (in the SN rest frame)

SNLS = supernova legacy survey

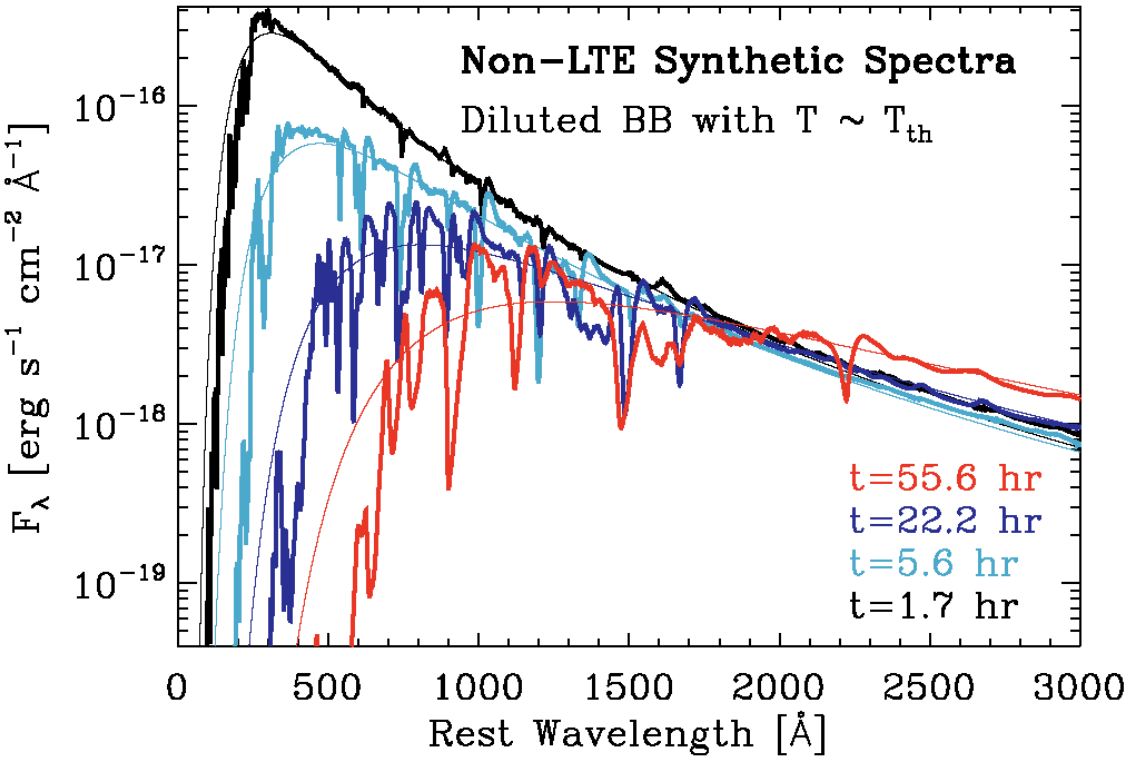

Kepler (15 Msun) plus CMFGEN models

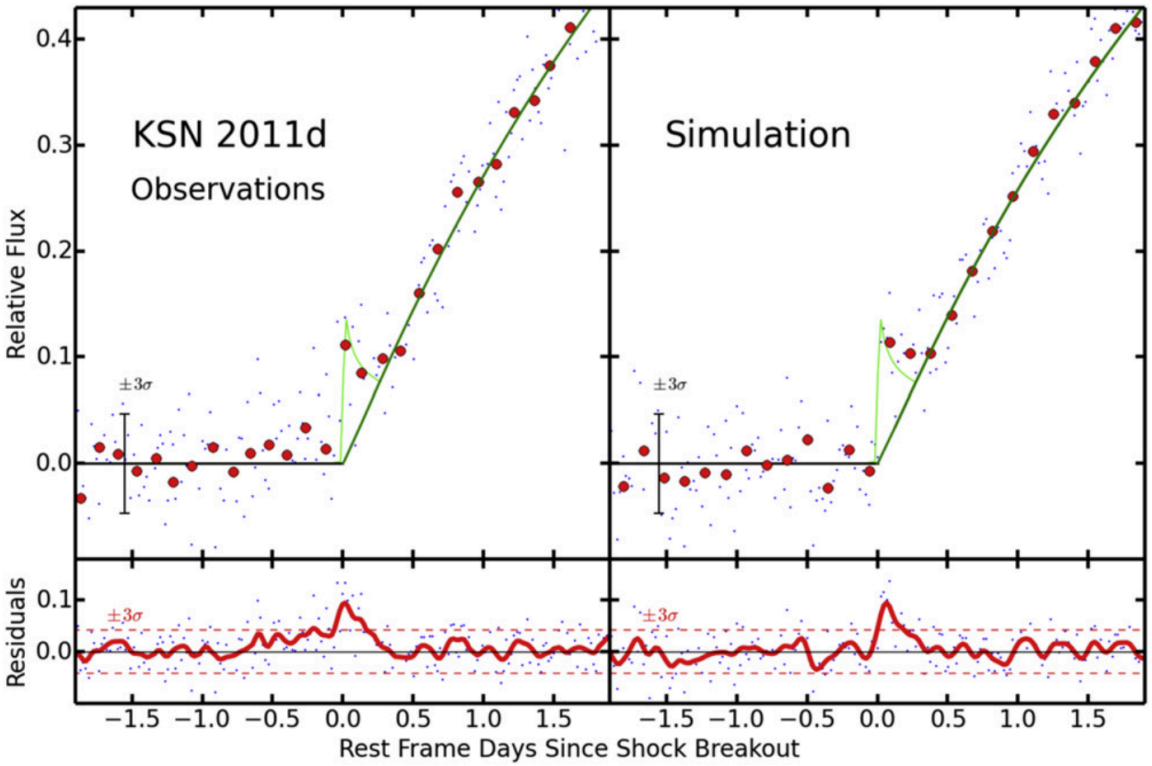

Figure 4. Left: the *Kepler* light curve of KSN2011d focused on the time expected for shock breakout. The blue dots are individual *Kepler* measurements and the red symbols show 3.5 hr medians of the *Kepler* data. An error bar at −1.5 days indicates the 3σ uncertainty on the median points. The green line shows the best fit photospheric model light curve. The lower panel displays the residuals between the observations and the model fit. The thick red line is a Gaussian smoothed residual light curve using a full-width at half-maxmimum of two hours. The dashed red lines indicate 3σ deviations of the Gaussian smoothed curve. The residual at the time expected for shock breakout is more than 5σ, implying that the feature is unlikely to be a random fluctuation. Right: a simulated light curve created using the statistical properties of the *Kepler* photometry and the best fit photospheric model. In addition, a Nakar & Sari (2010) shock breakout model (light green line) for an explosion energy of 2 B and radius of 490 $R_{\odot}$ is compared with both the data and simulation.

This is in the optical, far out on the tail of the spectrum of the hard uv burst. Lasts longer.

Pair-instability supernovae

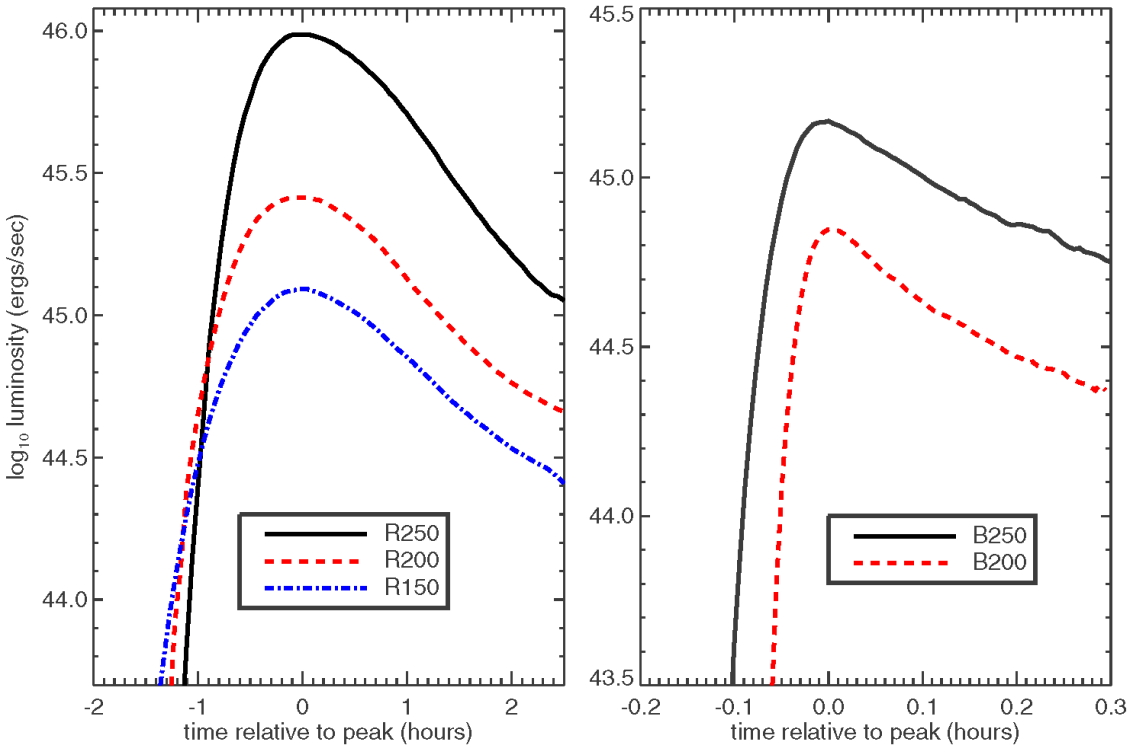

Figure 3. Calculated bolometric light curves of the shock breakout transient from pair instability explosions of massive red-supergiant (left) and blue-supergiant (right) stars. The duration of the burst, determined by the light crossing time, is significantly longer for the more extended red-supergiant models.

(A color version of this figure is available in the online journal.)

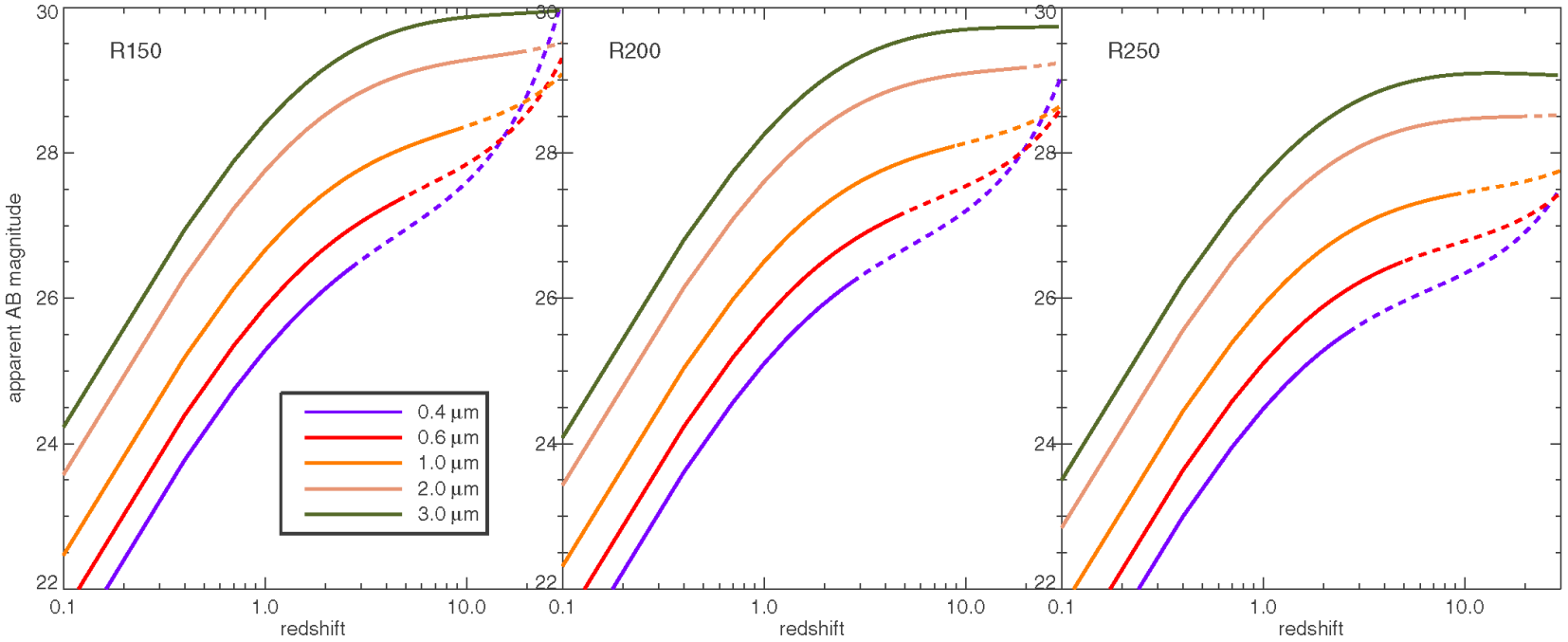

Figure 17. Detectability of the shock breakout transient from pair instability supernovae as a function of redshift. The figure plots the observed AB magnitude (for different wavelength bands) of three red-supergiant models at the peak of the bolometric breakout light curve. (Note an AB magnitude of 28.9 corresponds to 10 nJ.) Solid lines denote the redshift range for which the rest-frame flux is redder than 1216 Å (the Lyα line); at higher redshifts, the flux is likely absorbed by intervening neutral hydrogen (dashed lines). The breakout transients of the blue-supergiant models will be significantly dimmer than the models shown here, as the luminosity is lower and the spectrum peaks at much lower wavelengths.

Detectable to redshift 10 using JWST but small field of view implies a low event rate. May be detectable to z=10 by WFIRST.

2. The Plateau : Envelope Recombination

Over the next few days the temperature falls to ~5500 K, at which point, for the densities near the photosphere, hydrogen recombines. The recombination does not occur all at once for the entire envelope, but rather as a wave that propagates inwards in mass – though initially outwards in radius. During this time $R_{photo} \sim 10^{15} - 10^{16}$ *cm.*

The internal energy deposited by the shock is converted almost entirely to expansion kinetic energy. R has expanded by 100 or more (depending on the initial radius of the star) and the envelope has cooled dramatically.

$$T \propto \frac{1}{r} \qquad \rho \propto \frac{1}{r^3} \qquad \rho \propto T^3$$ (adiabatic with radiation entropy dominant)

$$\varepsilon \propto \frac{T^4}{\rho} \propto \frac{1}{r}$$

As a result only ~10^{49} erg (RSG; 10^{48} BSG) is available to be radiated away. The remainder has gone into kinetic energy, now ~10^{51} erg.

As the hydrogen recombines, the free electron density decreases and κ_{es} *similarly declines. (note analogy to the early universe)..*

H ionization - 15 solar masses. As the recombination front moves in the photospheric v declines. When the recombination reaches the He core the plateau ends

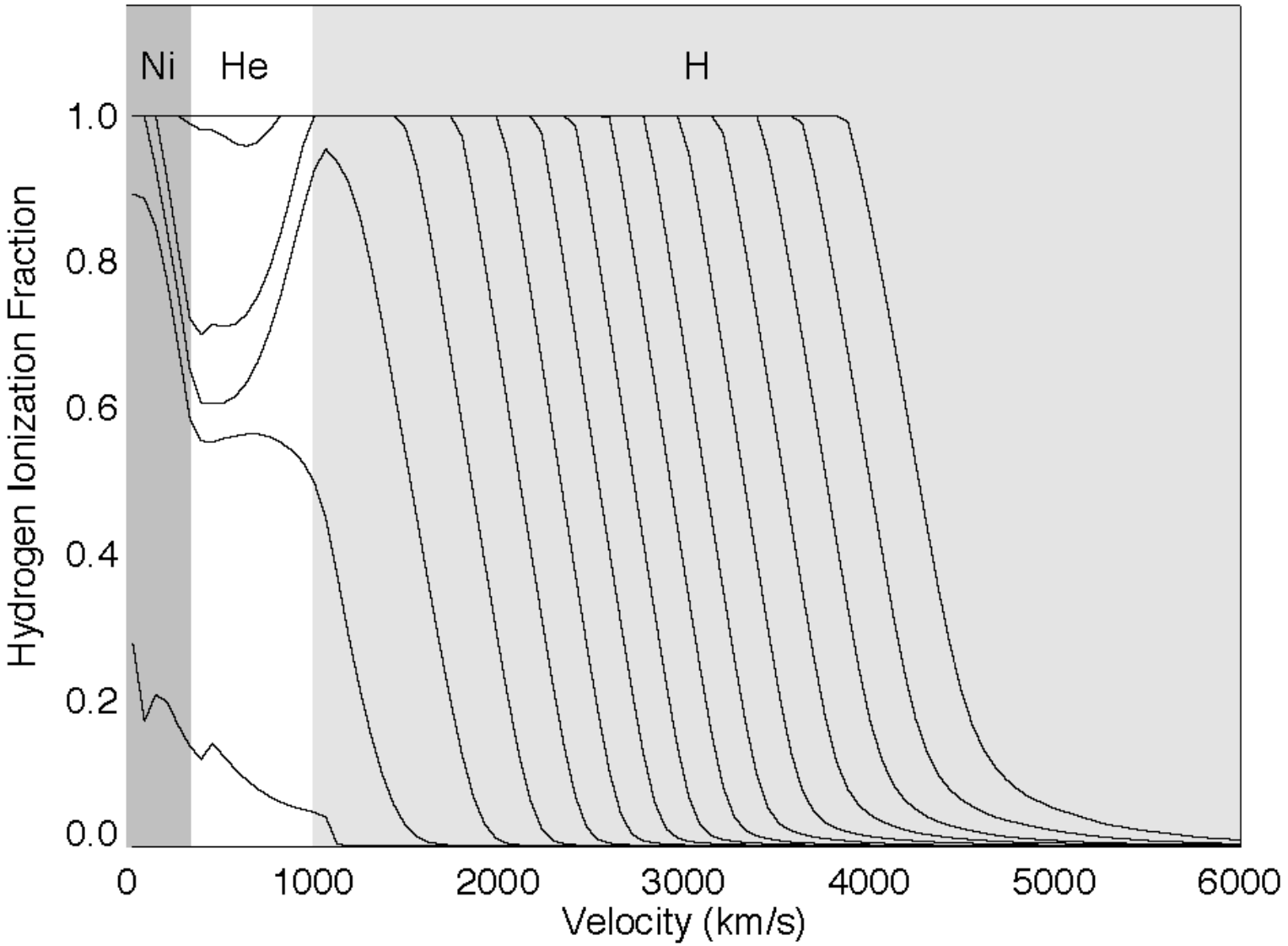

Photospheric speed

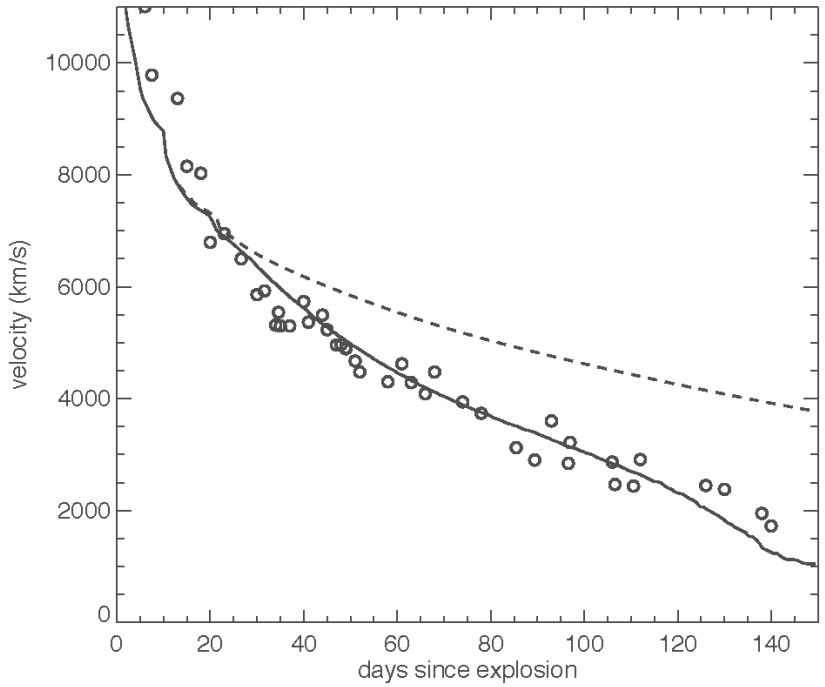

Kasen and Woosley (2009)

Fig. 4.— Photospheric velocity evolution of model M15_E1.2 as a function of time. The solid line shows the velocity of the electron scattering photosphere defined at $\tau_e = 2/3$. The dashed line shows the photospheric velocity in a model in which hydrogen recombination is neglected. The circles are the observed velocities of the sample of SNe IIP compiled by Nugent et al. (2006)

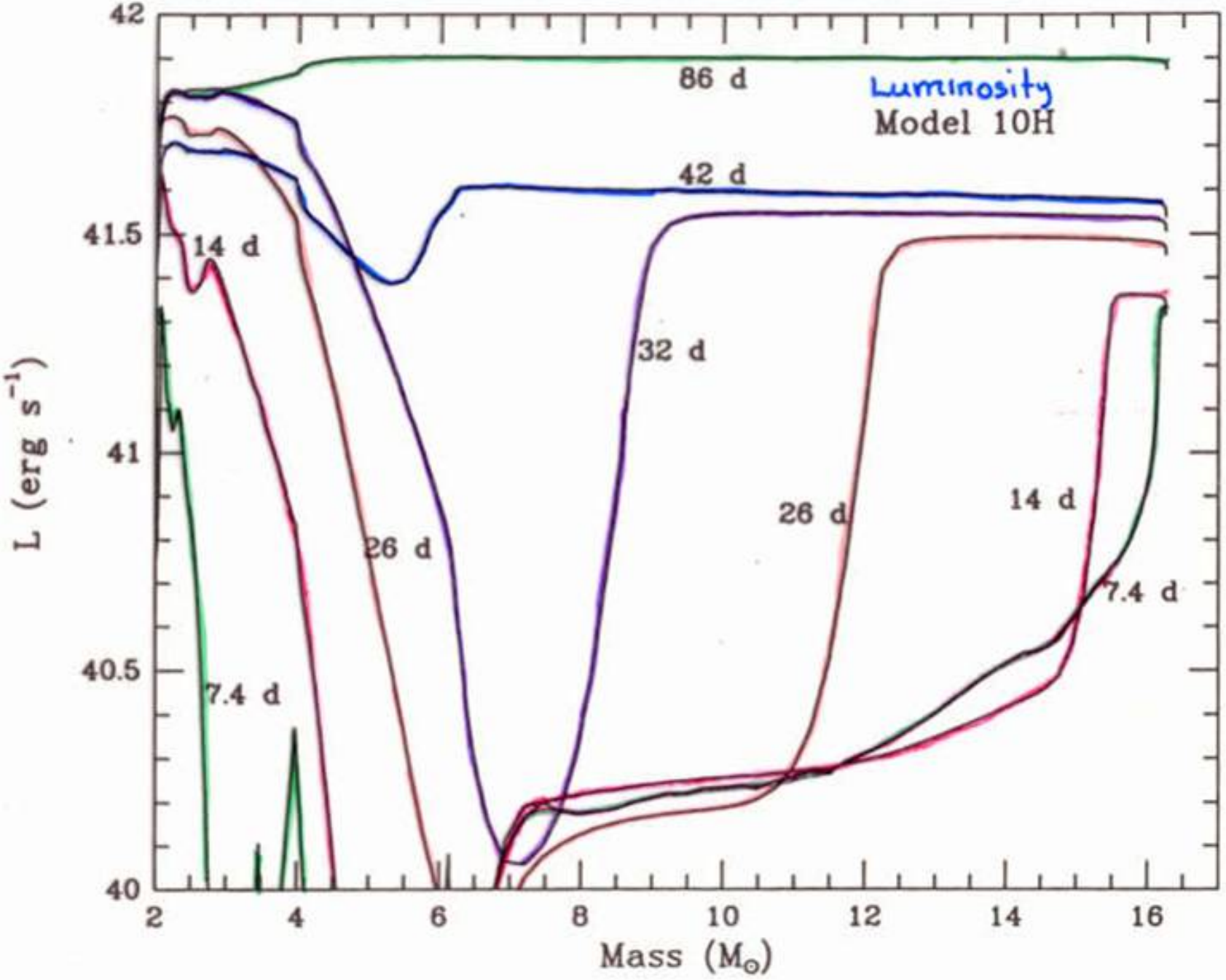
Luminosity
Model 10H
86 d
42 d
14 d
32 d
26 d
26 d
14 d
7.4 d
7.4 d
L (erg s^{-1})
Mass ($M_\odot$)
42
41.5
41
40.5
40
2
4
6
8
10
12
14
16

Popov (1993, *ApJ*, **414**, 712) gives the following scaling relations which he derives analytically:

$$t_{plateau} \approx 109\,\text{days}\,\frac{\kappa_{0.4}^{1/6}\,M_{10}^{1/2}\,R_{500}^{1/6}}{E_{51}^{1/6}\left(T_{ion}/4500\right)^{2/3}}$$

$$L_{bol} \approx 1.1\times10^{42}\,\frac{\text{erg}}{\text{s}}\,\frac{R_{500}^{2/3}\,E_{51}^{5/6}\left(T_{ion}/4500\right)^{4/3}}{M_{10}^{1/2}\,\kappa_{0.4}^{1/3}}$$

not quite linear in R because a more compact progenitor recombines at a slightly smaller radius.

where R_{500} is the radius of the preSN star in units of 500 $R_\odot$ (3.5×10^{13} cm);

$\kappa_{0.4}$ is the opacity in units of 0.4 $cm^2 gm^{-1}$

M_{10} is the mass of the hydrogen envelope (not the star) in units of 10 $M_\odot$

E_{51} is the kinetic energy of the explosion in units of 10^{51} erg

T_{ion} is the recombination temperature (5500 is better than 4500)

In fact the correct duration of the plateau cannot be determined in a calculation that ignores radioactive energy input.

Kasen and Woosley (2009) give:

$$L_{bol} \approx 1.26\times10^{42} \; \frac{R_{500}^{2/3} E_{51}^{5/6} X_{He,0.33}}{M_{10}^{1/2}} \; \text{erg s}^{-1}$$

where $X_{He,0.33}$ is the mass fraction of helium in the envelope divided by 0.33

Sukhbold et al (2016) give a semi-empirical formula for the plateau duration

$$t_{plateau} \approx 88\,\text{days} \; \frac{f_{rad}^{1/6} M_{10}^{1/2} R_{500}^{1/6}}{E_{51}^{1/6}}$$

where $f_{rad} = 1 + 21\frac{M_{Ni}}{E_{51}^{1/2} M_{10}^{1/2} R_{500}}$

II p

Ib, c

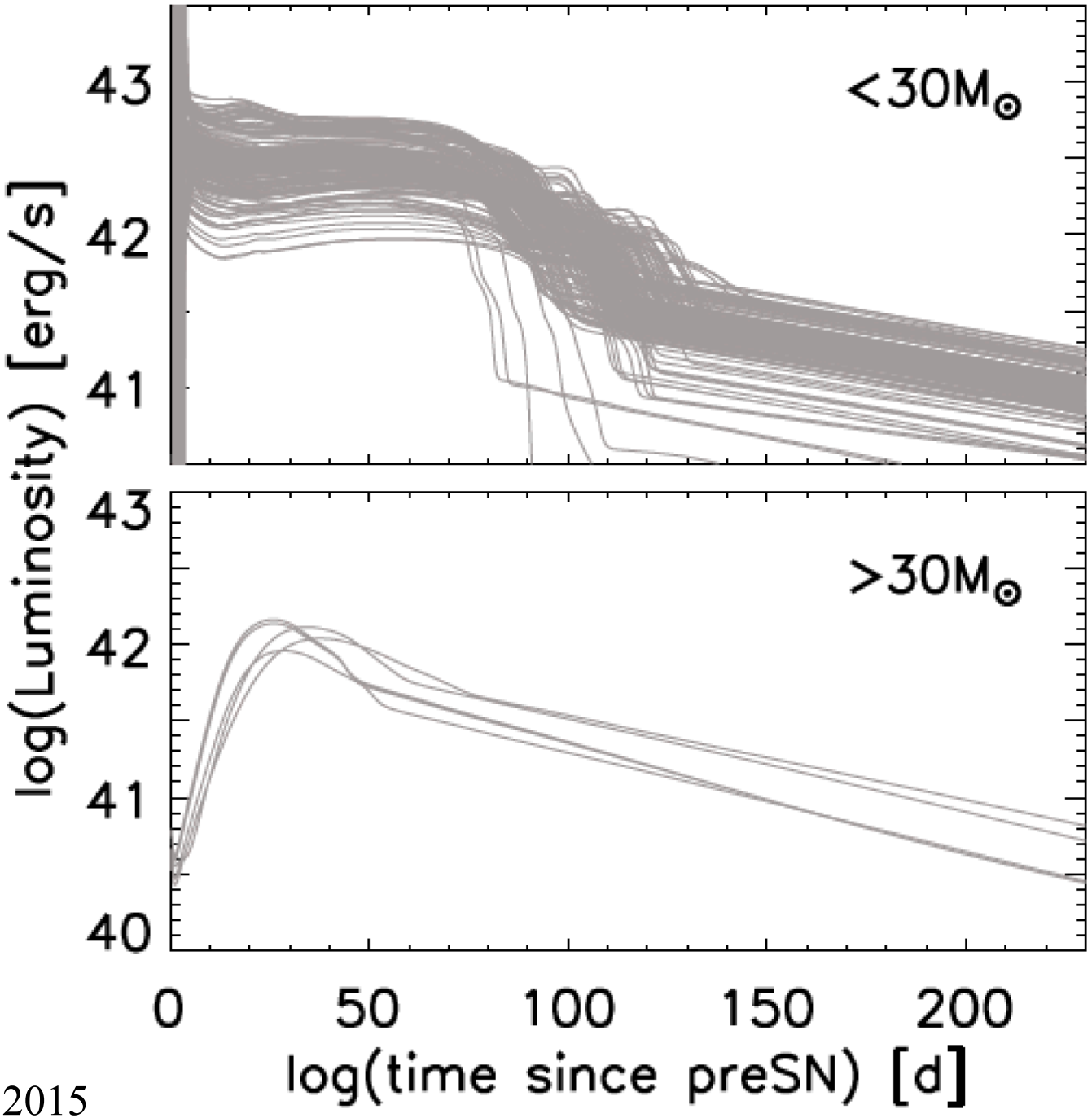

Sukhbold et al 2015

Pejcha and Prieto (2015)

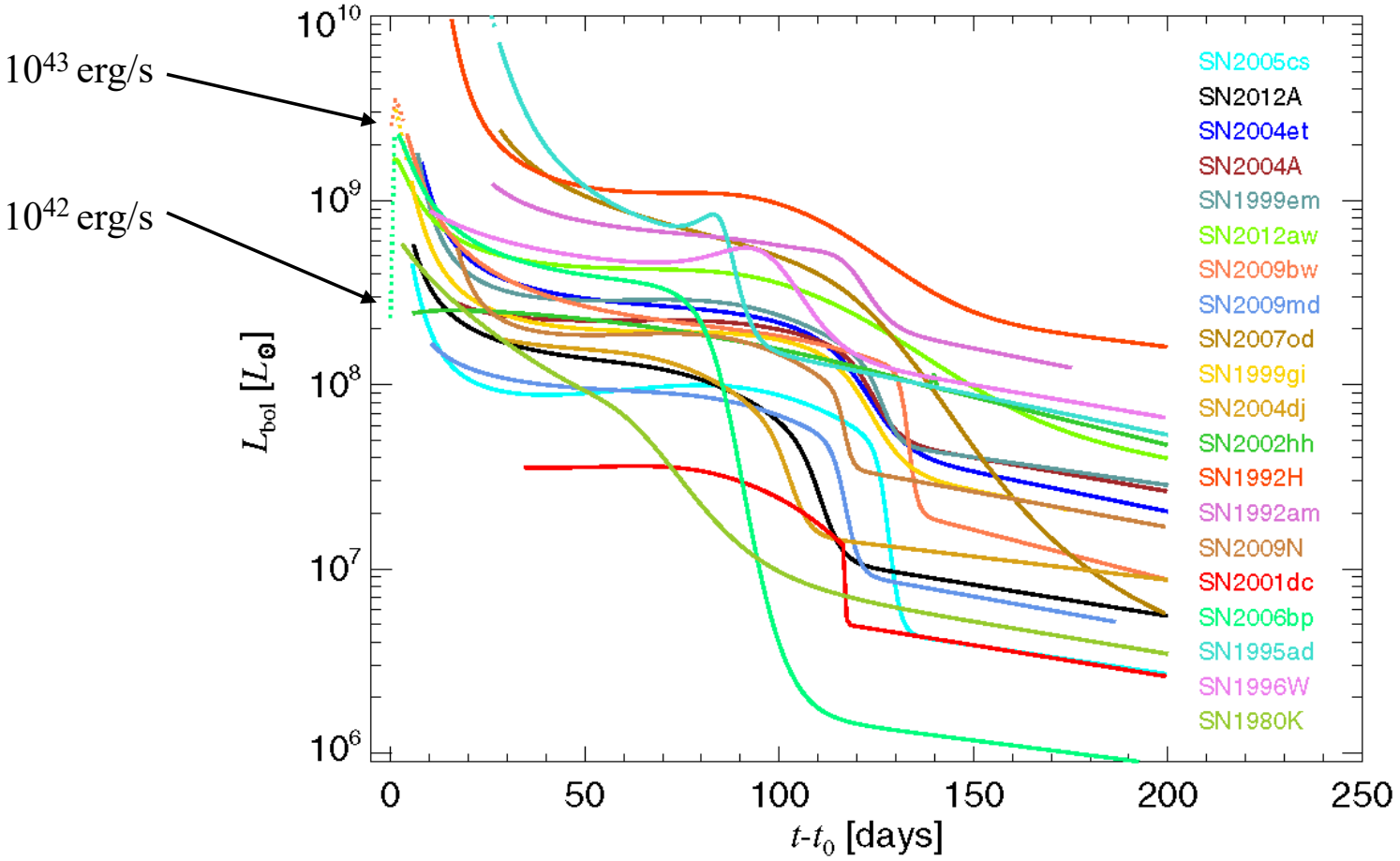

Figure 14. Bolometric luminosity as a function of time for supernovae with $\sigma_\mu < 0.2$ mag. The bolometric luminosity was calculated from the $UBVRIJHK$ bands combined with *Swift* bands $uvw2$, $uvm2$, $uvw1$, and u. For each supernova, we show $L_{\rm bol}$ between the first and last observation. Dotted segments of $L_{\rm bol}$ mark the temperatures not constrained by *Swift* data ($\tau < 0.095$).

Cosmology on the Plateau
Baade-Wesselink Method
(aka "The Expanding Photosphere Method (EPM)

$$\phi = \frac{L}{4\pi D^2} = \frac{4\pi R_{ph}^2 \sigma T_e^4}{4\pi D^2} \qquad D = \text{distance}$$

$$D = R_{ph} T_e^2 \left(\frac{\sigma}{\phi} \right)^{1/2}$$

$$R_{ph} = R_{ph}^0 + v_{ph}(t - t_0)$$

can ignore R_{ph}^0

Measure on two or more occasions, $t_i \quad - v_i, T_i,$ and ϕ_i

Solve for D and t_0.

In reality, the color temperature and effective temperature are not the same and that requires the solution of a model to obtain a "diluion factor". But the physics of the plateau is well understood. This is a first principles method of getting distances. No Cepheid calibration is necessary - though it is useful to have one.

Eastman, Schmidt, and Kirshner (1996)
give the dilution factor for a set of models

$H_0 = 73 \pm 7$

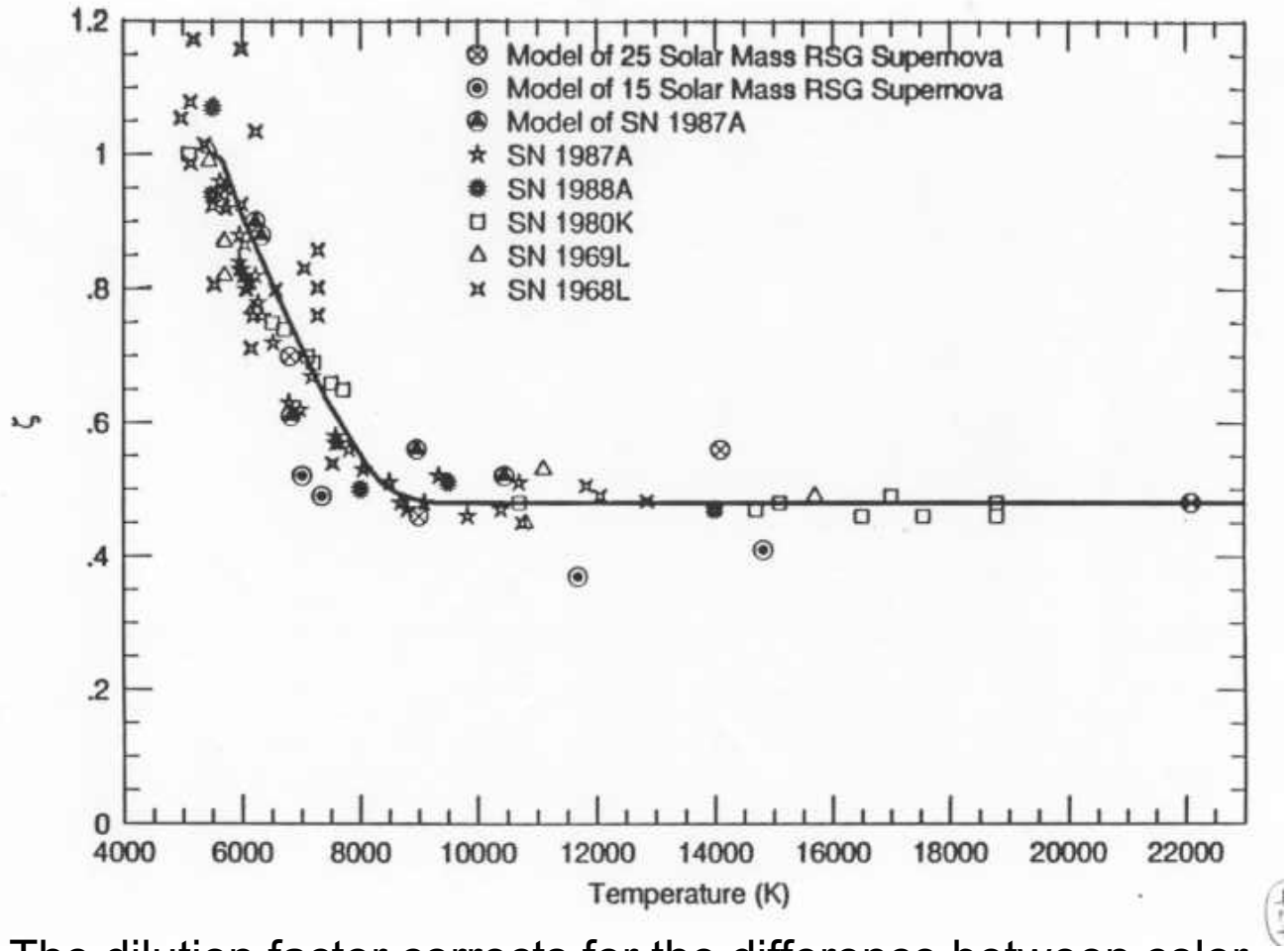

The dilution factor corrects for the difference between color temperature and effective temperature and also for the finite thickness of the photosphere which leads to a spread in T. See Dessart and Hillier (A&A, 2005), Bose and Kumar (2014)

Problems using EPM

- Uncertainties in dilution factors (+- 0.1 common)
- Difficulty knowing which lines to use (Fe)
  and when to apply (earlier is better, < 50 days). v uncertain to 10%
- Extinction, metallicity effects (around 7% - Hamuy et al)
- Good for 87A but differs from Cepheid distance for SN 1999em
  by 50% at early times (< 1 week; Hamuy et al 2001)
- Requires spectra for velocities – not just photometry
- Can be improved using spectrum fitting (Baron et al 2004)
  (20% accuracy for distances). Don't need dilution factor
  but still use a model

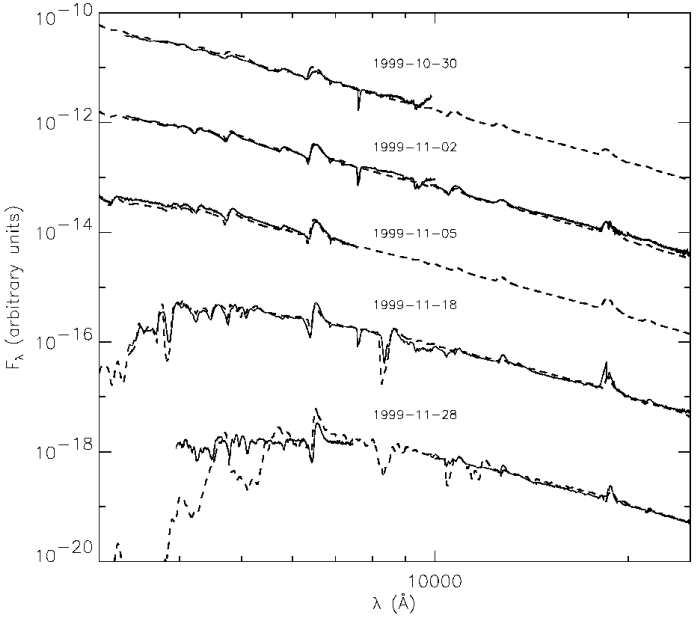

Baron et al (2004)
SN 1999em

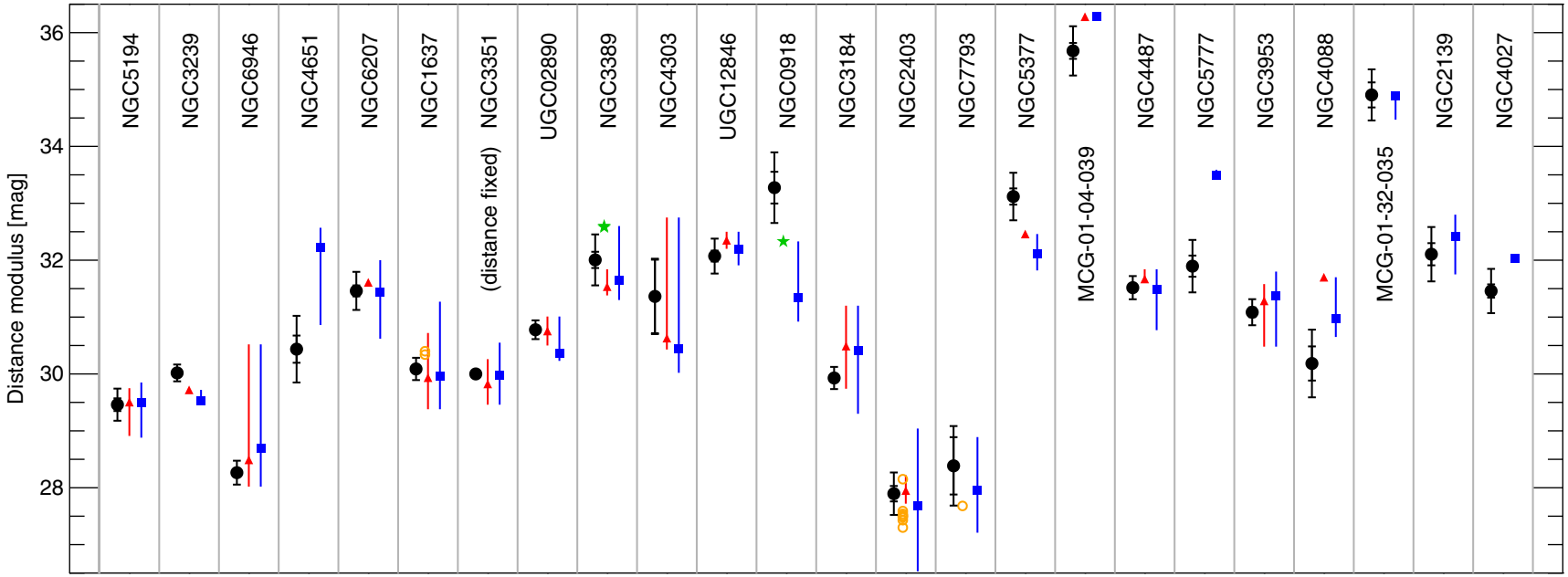

Figure 11. Comparison of the distance estimates of galaxies in our sample (solid black circles with 1σ uncertainties of the original fit and the modified fit with $\mathcal{H}/N_{\rm DOF} = 1$) to the data in NED: median values of either Type II supernovae only or all distance estimates are shown with solid red triangle or blue square, respectively, while the full range of measurements is shown with vertical colored lines. For a few galaxies, we highlight individual distance measurements with Cepheids (open orange circles) or with supernovae Ia (solid green stars). Distances of Type II supernovae are from Baron et al. (1996, 2007), Bartel (1988), Bose & Kumar (2014), Dessart & Hillier (2006); Dessart et al. (2008), Elmhamdi et al. (2003), Fraser et al. (2011), Hamuy et al. (2001), Hendry et al. (2006), Inserra et al. (2012a), Iwamoto et al. (1994), Jones et al. (2009), Leonard et al. (2002a, 2002b, 2003), Olivares E. et al. (2010), Poznanski et al. (2009), Richmond et al. (1996), Roy et al. (2011), Sahu et al. (2006), Schmidt et al. (1992, 1994a, 1994b), Sparks (1994), Takáts et al. (2014); Takáts & Vinkó (2006, 2012), Tomasella et al. (2013), Vinkó et al. (2006, 2012), Weiler et al. (1998), of Cepheids are from Freedman & Madore (1988), Freedman et al. (2001), Humphreys et al. (1986), Leonard et al. (2003), Madore & Freedman (1991), McAlary & Madore (1984), Metcalfe & Shanks (1991), Pietrzyński et al. (2010), Saha et al. (2006), and of Type Ia supernovae from: Maguire et al. (2012), Parodi et al. (2000).

Pejcha and Prieo (2015) give no estimate of the accuracy of their combined EPM and spectral method, but 0.2 magnitudes corresponds to about 10% in distance.

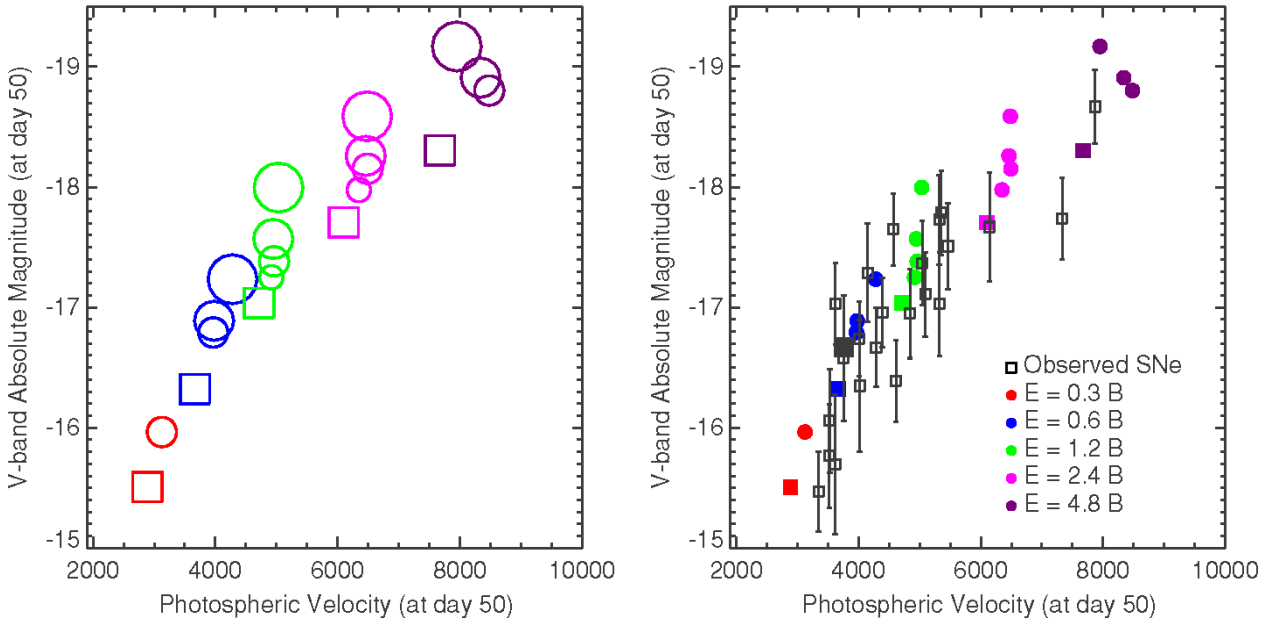

Figure 16. Model SC relationship between the *V*-band plateau luminosity (measured at 50 days) and the photospheric velocity. Left: the models are color coded by explosion energy. Circles denote solar metallicity models, squares 0.1 solar models, and the size of the symbol is proportional to the progenitor star mass. Right: comparison of the model relation (circles) with the observation sample compiled by Hamuy (2003; open squares). The large filled square is SN 1999em using the Cepheid distance of Leonard et al. (2003) and an extinction of $A_v = 0.31$.

Bottom line: SN Iip are probably good for getting distances ~10% but in an era of precision cosmology that may not suffice.

Light Curve Tail Powered by Radioactive Decay

a) $^{56}Ni\ (e^-, \nu_e)\ ^{56}Co$ + 1.72 MeV in γ-rays

$\tau_{1/2} = 6.1$ d

$\epsilon_\gamma = 3.0 \times 10^{16}$ erg/gm

b) $^{56}Co\ (e^-, \nu_e)\ ^{56}Fe$ 81%

and $(e^+ \bar{\nu}_e)\ ^{56}Fe$ 19%

+ 3.72 MeV in γ-rays

$\tau_{1/2} = 77.1$ d $\quad 6.4 \times 10^{16}$ erg/gm

In 0.07 $M_\odot$ of $^{56}Ni \rightarrow {}^{56}Fe$ 1.3×10^{49} erg is released.

Implications for light curve and dyamics.

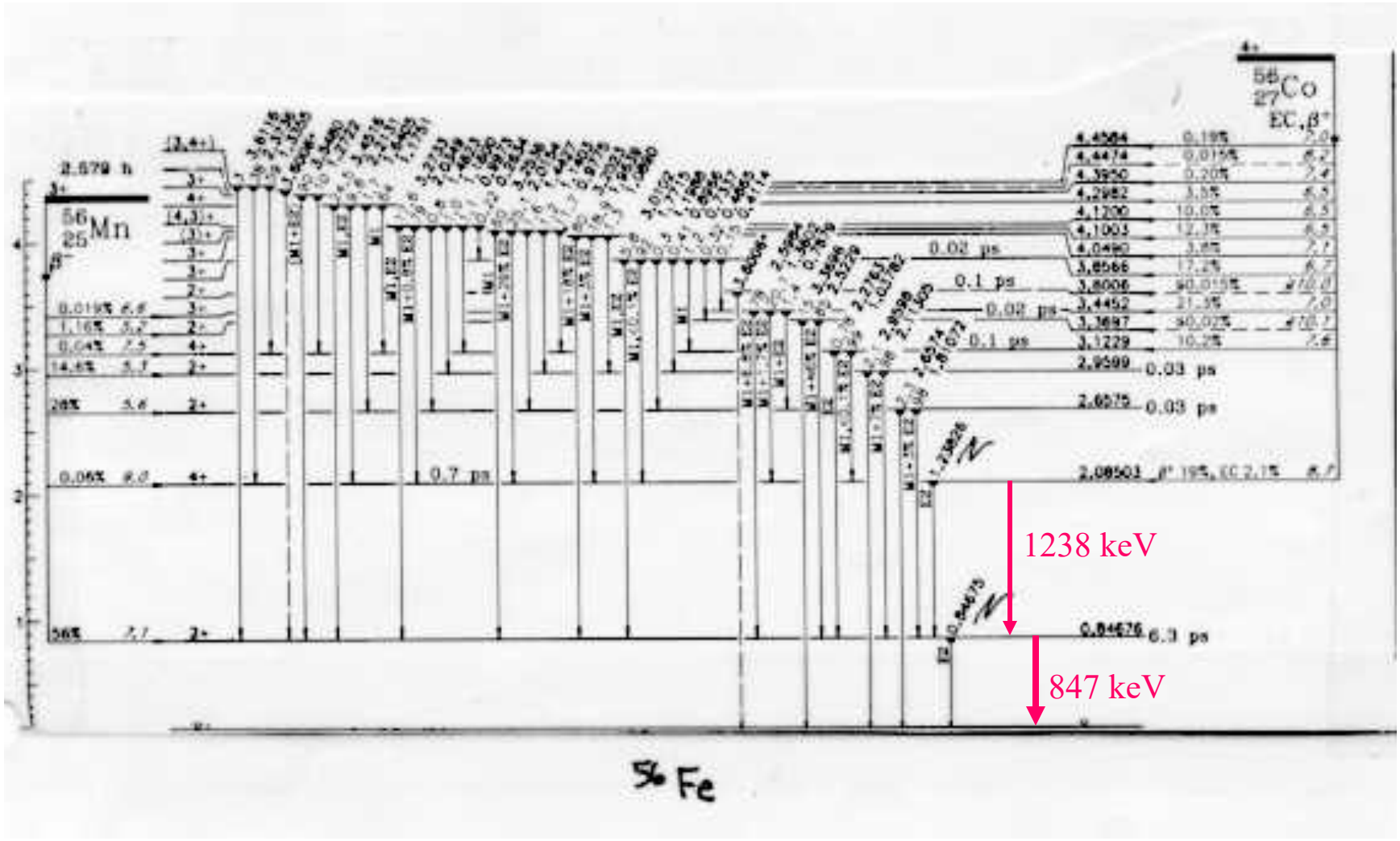
56 25 Mn
2.579 h
56 27 Co
EC, β+
0.7 ps
0.02 ps
0.1 ps
0.02 ps
0.1 ps
0.03 ps
0.03 ps
1238 keV
847 keV
6.3 ps
56 Fe

As mentioned previously, radioactivity lengthens the light curve since it continues to supply fresh energy at late time when the adiabatic degradation is small

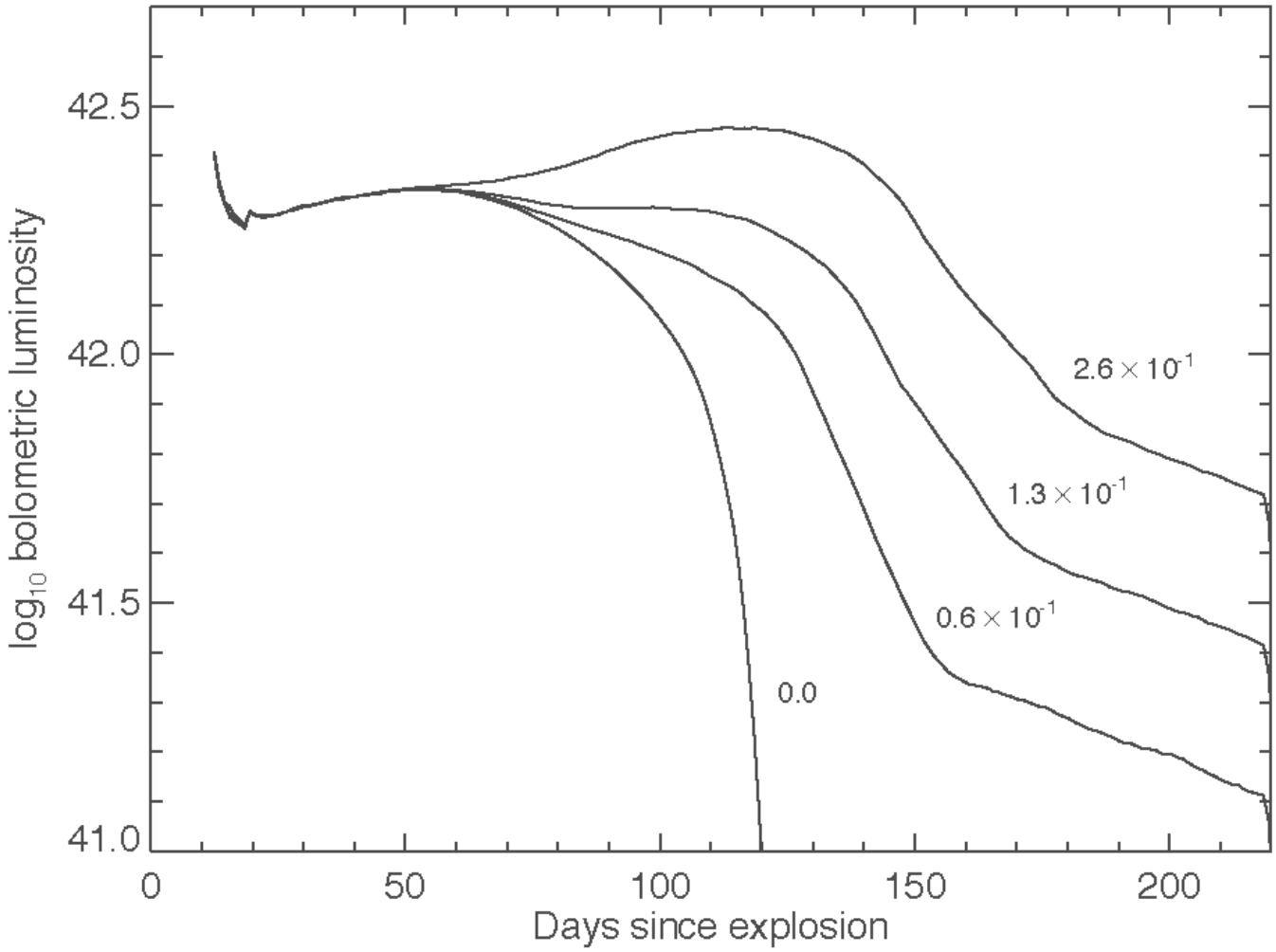

1.2 B explosion of 15 solar mass RSG with different productions of ^{56}Ni indicated by the labels. Kasen et al. (2009)

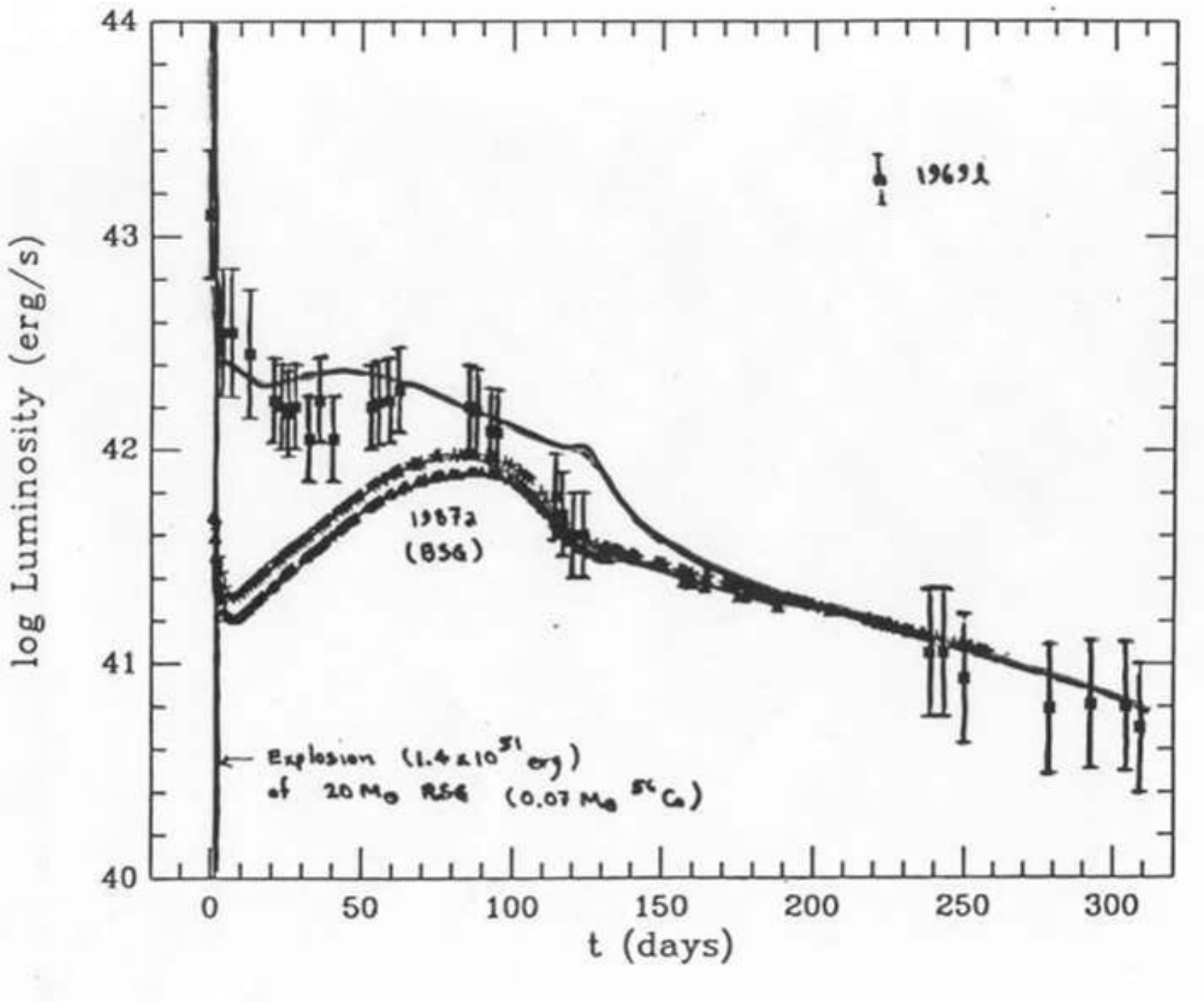
log Luminosity (erg/s)
44
43
42
41
40
0
50
100
150
200
250
300
t (days)
1969L
1987A
(BSG)
← Explosion (1.4 x 10^51 erg)
of 20 M⊙ RSG (0.07 M⊙ 56Co)

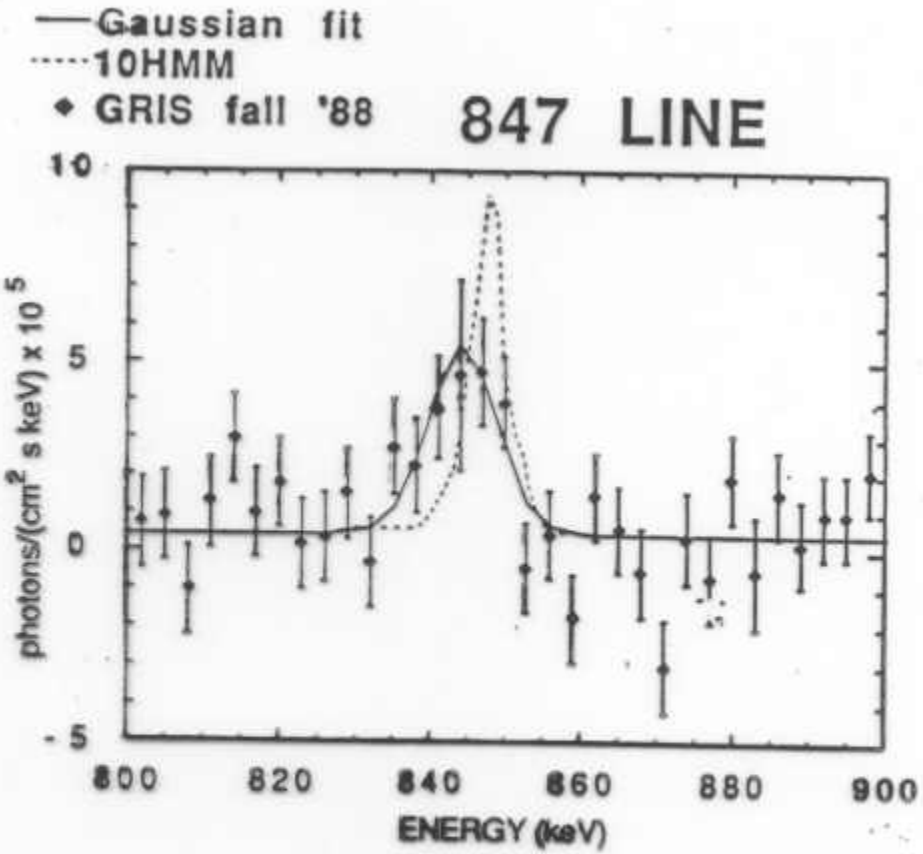

Figure 2. GRIS data for the 847 keV line from the decay of ^{56}Co in SN87A is shown for day 613. The top-of-atmosphere photon spectrum is shown in 3 keV bins which are larger than the FWHM resolution of the instrument. The solid line is a best fit to a Gaussian line profile. The dashed line is the predicted line profile for the 10HMM model. Although this model and similar spherically symmetric mixed models predict the line flux correctly there is a clear discrepancy with the measured line profile.

Other short lived radioactivites of interest:

$^{57}\mathrm{Co}(e^-,\bar{\nu}_e)^{57}\mathrm{Fe}$ $\quad\quad$ $\tau_{1/2} = 272$ days

$^{44}\mathrm{Ti}(e^-,\bar{\nu}_e)^{44}\mathrm{Sc}$ $\quad\quad$ $\tau_{1/2} = 60$ years

$^{44}\mathrm{Sc}(e^-,\bar{\nu}_e)^{44}\mathrm{Ca}$ $\quad\quad$ = 2.44 days

$^{44}\mathrm{Sc}(e^+\nu_e)^{44}\mathrm{Ca}$

The effect of ^{57}Co decay on the light curve of SN1987A was observed. ^{44}Ti hs been detected in both the Cas A SNR (Iyudin et al 1996) and SN1987A (Boggs et al, 2015).

The amount of ^{44}Ti seen in both cases was just over 10^{-4} $M_\odot$ which is a bit larger than most predictions. The motion also indicates assymetry in the explosion

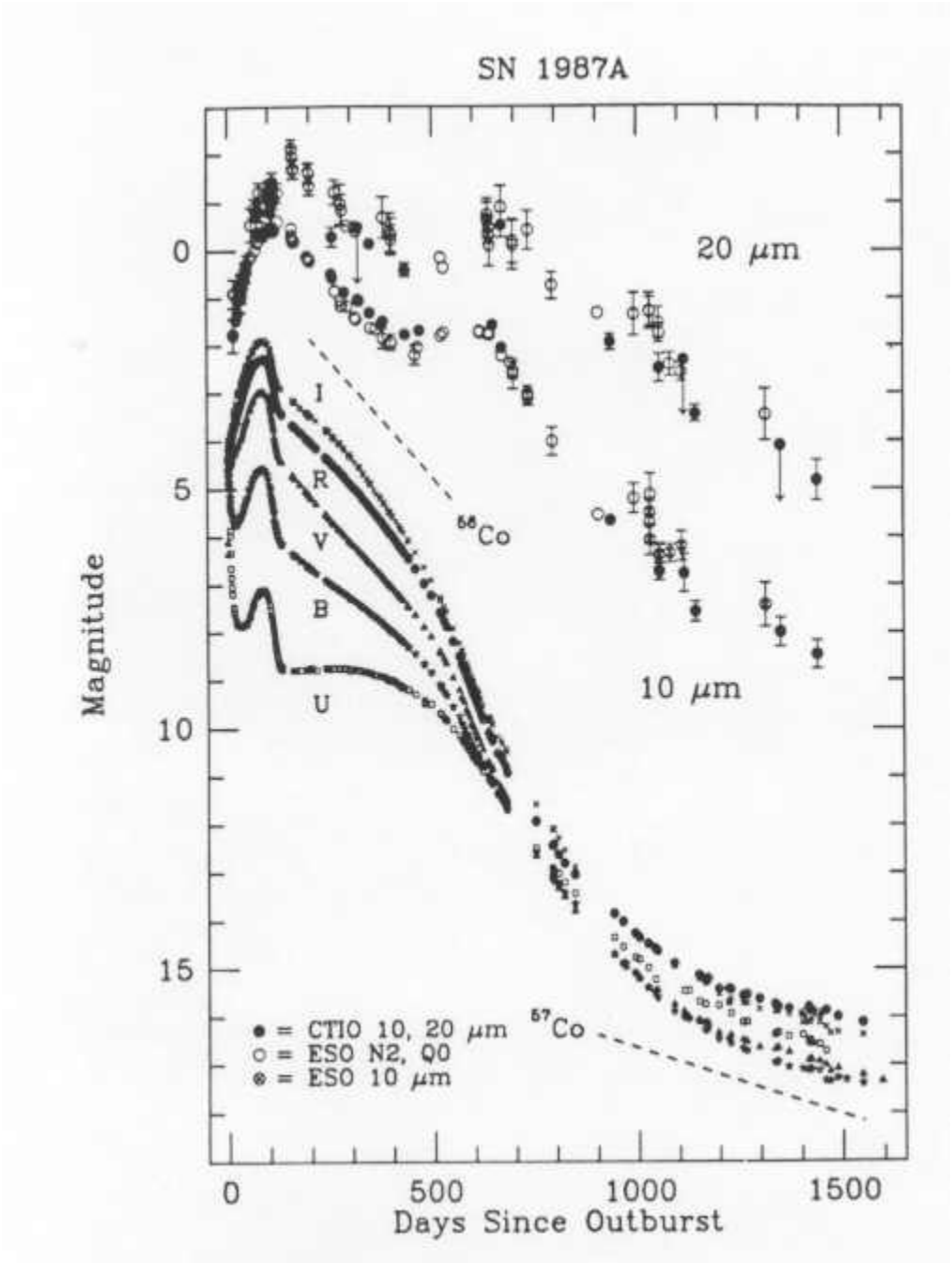
SN 1987A
20 μm
10 μm
I
R
V
B
U
^{56}Co
^{57}Co
● = CTIO 10, 20 μm
○ = ESO N2, Q0
⊗ = ESO 10 μm
Magnitude
0
5
10
15
0
500
1000
1500
Days Since Outburst

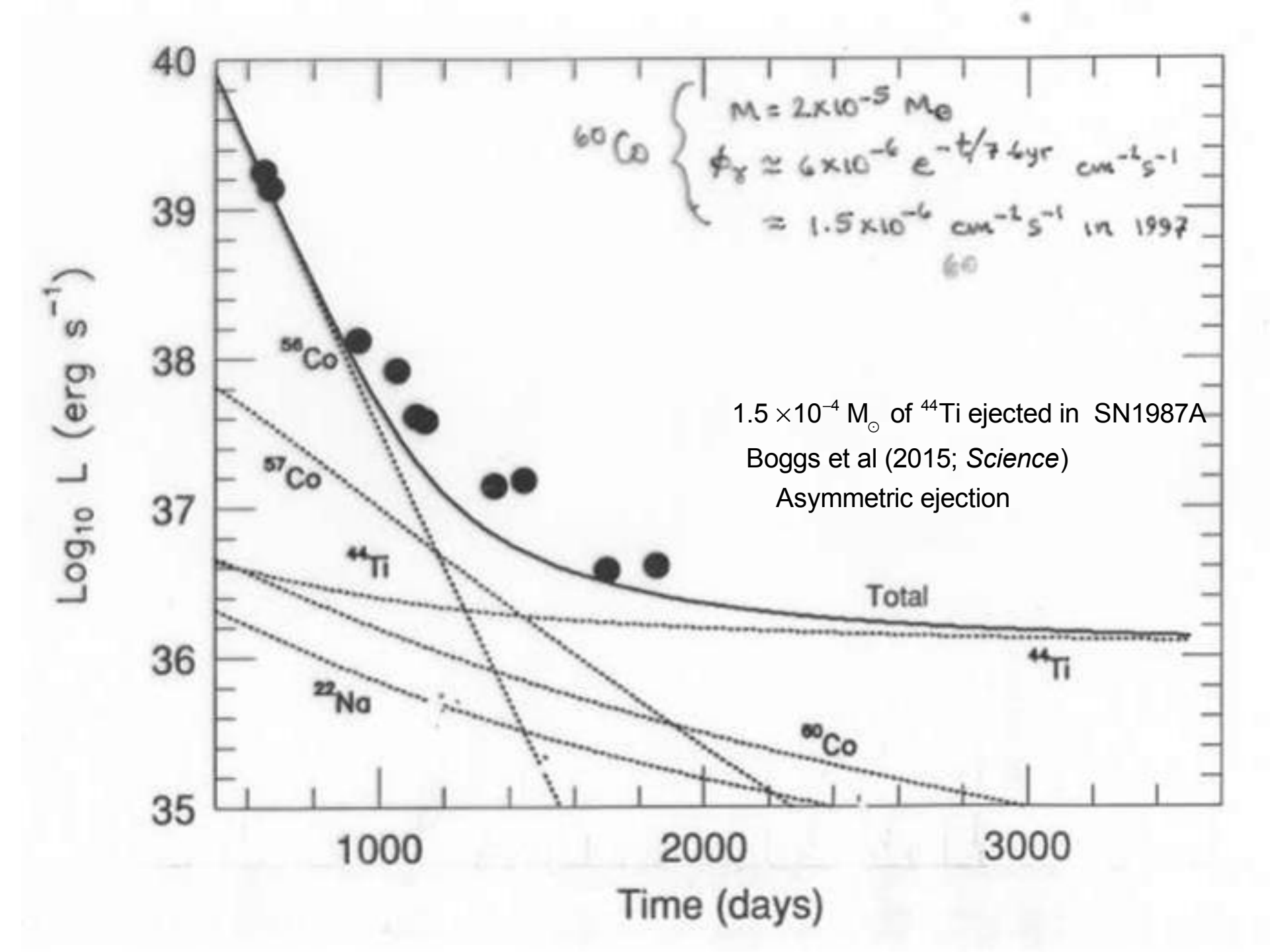
40
39
38
37
36
35
Log10 L (erg s-1)
1000
2000
3000
Time (days)
56Co
57Co
44Ti
22Na
60Co
Total
44Ti
60Co
M = 2x10-5 M⊙
φγ ≈ 6x10-6 e-t/7.6yr cm-2s-1
≈ 1.5x10-6 cm-2s-1 in 1997
1.5 ×10−4 M⊙ of 44Ti ejected in SN1987A
Boggs et al (2015; Science)
Asymmetric ejection